1995MNRAS.276..796S

Mon. Not. R. Astron. Soc. **276**, 796–824 (1995)

Merging and hierarchical clustering from an initially Poisson distribution

Ravi K. Sheth
Berkeley Astronomy Department, University of California, Berkeley, CA 94720, USA

Downloaded from https://academic.oup.com/mnras/article/276/3/796/1034602 by U.S. Department of Justice user on 17 August 2022

Accepted 1995 April 25. Received 1995 April 12; in original form 1994 November 14

ABSTRACT

The excursion set, Press–Schechter mass spectrum for a Poisson distribution of identical particles is derived. For the special case of an initially Poisson distribution the spatial distribution of the Press–Schechter clumps is shown to be Poisson. Thus, the distribution function of particle counts in randomly placed cells is easily obtained from the Press–Schechter multiplicity function. This Poisson Press–Schechter distribution function has the same form as the well-studied gravitational quasi-equilibrium counts-in-cells distribution function which fits the observed galaxy distribution well.

The description of merging and hierarchical clustering from an initially Poisson distribution is also formulated and solved. These solutions represent the discrete analogue of those already obtained for an initially Gaussian distribution. In addition, physically motivated arguments are used to provide insight about the structure of the partition function that describes all possible merger histories. From this partition function an expression for the number of progenitor clumps as a function of cluster size is obtained. This, with the knowledge that initially Press–Schechter clumps have a Poisson spatial distribution, is used to calculate the subsequent clustering of these clumps. Thus, the growth of hierarchical clustering on all levels of the hierarchy is quantified. Comparison of the analytic results with relevant N-body simulations of gravitational clustering shows substantial agreement.

A method for extending all these results to describe the growth of clustering from more general, non-Gaussian, compound Poisson distributions is also described. For these compound Poisson processes a scaling relation is obtained that greatly clarifies the results of relevant N-body simulations in which particles have a range of masses. This scaling solution and the merger history results are consistent with a simple model of the growth of hierarchical clustering. At early times in this model, clustering on all levels of the hierarchy is well approximated by appropriately renormalized Poisson Press–Schechter forms.

Key words: galaxies: clustering – galaxies: evolution – galaxies: formation – cosmology: theory – dark matter.

1 INTRODUCTION

The distribution function,

$$P(N,\bar{n}V)=\frac{\bar{N}(1-b)}{N!}\left[\bar{N}(1-b)+Nb\right]^{N-1}\mathrm{e}^{-\bar{N}(1-b)-Nb}, \tag{1}$$

where $P(N,\bar{n}V)$ denotes the probability a randomly placed cell of size V has exactly N particles, $\bar{n}$ is the average number density of particles (so that $\bar{N}=\bar{n}V$ is the average number of particles in a cell), and b is a free parameter with $0\leqslant b\leqslant 1$, was first proposed by Saslaw & Hamilton (1984). Equation (1) derives from their specific thermodynamic model of non-linear gravitational clustering. Although in their model b was supposed independent of scale, most comparisons of this functional form with counts-in-cells analyses of galaxy catalogues and N-body simulations show good agreement provided b is allowed to depend (quite strongly) on scale. When treated purely as a fitting function in this way, equation (1) provides a good fit to counts-in-cells distribution functions

© Royal Astronomical Society • Provided by the NASA Astrophysics Data System

1995MNRAS.276..796S

calculated for a number of two- and three-dimensional galaxy catalogues (e.g. Saslaw & Crane 1991; Lahav & Saslaw 1992; Sheth, Mo & Saslaw 1994), and to simulations of gravitational clustering from Poisson initial conditions (e.g. Itoh, Inagaki & Saslaw 1993 and references therein).

A number of analytic properties of this distribution function are derived by Hamilton, Saslaw & Thuan (1985), Saslaw (1989), and Sheth (1994). Of particular importance in the present work is the cluster decomposition of equation (1). When b is independent of scale, Saslaw (1989) shows that equation (1) is a compound Poisson distribution, so that it can be understood as describing a distribution of randomly distributed point-shaped clusters (i.e., idealized clusters having no spatial extent). For equation (1), the probability, $\eta(N,b)$, that a randomly placed cluster has exactly N particles is given by the Borel distribution; i.e.,

$$\eta(N,b)=\frac{(Nb)^{N-1}\,\mathrm{e}^{-Nb}}{N!}. \tag{2}$$

Since the first moment of the Borel distribution is $1/(1-b)$ (e.g. Moran 1984; Saslaw 1989), this Borel decomposition shows that, when the mean density of particles is $\bar{n}$, then the mean number density of clusters having exactly N associated particles is $\bar{n}(1-b)\,\eta(N,b)$. The extension to models in which the Poisson-distributed clusters have some non-trivial shape and density profile is developed by Sheth & Saslaw (1994).

As mentioned above, equation (1) can be obtained from the thermodynamic model of gravitational clustering developed by Saslaw & Hamilton (1984). To solve their problem, and so to specify the subsequent thermodynamics and the resulting counts-in-cells distribution function, required that they make a guess regarding the functional form of the ratio of the gravitational energy of correlations to the kinetic energy associated with peculiar motions. This is equivalent to the guess (e.g. Davis & Peebles 1977; Hamilton 1988) that must be made to close and solve the BBGKY hierarchy. To date, there is little physical motivation to justify their guess (Sheth 1994), so it remains an ad hoc assumption in their model. Nevertheless, equation (1) appears to provide a reasonably, and perhaps unexpectedly, accurate description of the observations and simulations. Given the ad hoc nature of its derivation, however, it is important to be cautious about inferring anything about the accuracy and applicability of the thermodynamic approach from this demonstrated accuracy of equation (1).

This paper considers the excursion set mass spectrum (cf. Bond et al. 1991) of a Poisson distribution to provide a new derivation of equation (1). First, Section 2.1 uses the approach of Press & Schechter (1974) to describe the non-linear gravitational clustering of an initially Poisson distribution. It provides two alternative derivations of the probability that a cluster has a given number of particles, the cluster multiplicity function. The first derivation is due to Epstein (1983), and the second is new. Section 2.2 shows that if these Press–Schechter clusters are assumed to be idealized, point-sized clusters, and the clusters are assumed to have a Poisson spatial distribution, then the counts-in-cells distribution function of this set of Poisson-distributed Press–Schechter clumps is exactly the same as equation (1).

Insofar as the Press–Schechter approach is independent of an underlying thermodynamic theory, this derivation of equation (1) is effected without any explicit consideration of thermodynamics. Indeed, all the results of this paper apply whether the thermodynamic approach is valid or not. The Press–Schechter derivation of Section 2 also shows why equation (1) provides a good fit to counts-in-cells distribution functions measured in simulations of gravitational clustering from Poisson initial conditions, but is not so accurate when the initial conditions are significantly different from Poisson (e.g. Suto, Itoh & Inagaki 1990). Section 2.3 uses a linear theory calculation of the variance to calculate the time evolution of this Press–Schechter multiplicity function. The calculation is valid for cosmologies with arbitrary values of the density parameter, Ω, and is independent of the details of the assumed model of spherical collapse.

In Section 3 these results are generalized to calculate the excursion set mass functions of compound Poisson cluster models. Although the solution for the general compound Poisson cluster model is complex (Section 3.1), the excursion set mass spectrum for the compound Poisson cluster model that equation (1) describes exhibits a scaling property that greatly simplifies the Press–Schechter type description of non-linear clustering in it (Section 3.2). This scaling solution justifies the assumption of Section 2.2, that the Poisson Press–Schechter clumps have a Poisson distribution in space. The excursion set mass spectrum for the Negative Binomial distribution is derived in Section 3.3. The scaling solution found in Section 3.2, with the good agreement of the Borel decomposition and the physical clusters in the N-body simulations of gravitational clustering of identical particles in an expanding universe (Section 5), suggests a simple model for the evolution of hierarchical clustering from Poisson initial conditions. This model, developed in Section 3.4, assumes that clustering develops through a series of Poisson cluster distributions, and that, to a good approximation, clustering on every level of the hierarchy is described by the functional form of equation (1).

In Section 4 the Press–Schechter model developed in Section 2 is extended to formulate and solve for a more precise description of merging and hierarchical clustering from an initially Poisson distribution. Sections 4.1 and 4.2 use the techniques developed by Bond et al. (1991) and by Lacey & Cole (1993) for describing the development of clustering from an initially Gaussian field. Thus, the results of Sections 4.1 and 4.2 represent the discrete analogue of those already obtained for a Gaussian random field. In the appropriate limit, the expressions derived here reduce to those that describe merging in a white noise Gaussian random field.

Section 4.3 extends the analysis and provides a description of the entire merger history tree. The main result of this section concerns what is essentially a partition function that describes all possible merger histories of an initially Poisson distribution. It shows that this partition function can be calculated by assuming that the functional dependence on the initial and final epochs

Downloaded from https://academic.oup.com/mnras/article/276/3/796/1034602 by U.S. Department of Justice user on 17 August 2022

© Royal Astronomical Society • Provided by the NASA Astrophysics Data System

1995MNRAS.276..796S

of the probability that a particular tree structure occurs is the same for all choices of epochs. This assumption is consistent with what is already known about the Press–Schechter description – namely, for all choices of the epochs t_1 and t_2 for which $t_1 \geqslant t_2$, statements that describe the relation between t_1 and t_2 depend only on those two epochs, and not on what happened earlier than t_1 or will happen later than t_2 (Bower 1991; Bond et al. 1991).

Section 4.3 shows that this assumption leads to a physically reasonable merger model, in which, in the limit of very small time steps, the probability that a clump has two progenitors is an infinitesimal, the probability it has three progenitors is an infinitesimal of the next higher order, and so on. In the opposite limit of very large time steps, the probability that a large clump has only two progenitor clumps is smaller than the probability that it has three, and so on. Furthermore, for any given halo size, this assumption specifies the distribution of the number of progenitor clumps as a function of redshift, completely. This expression for the number of progenitor clumps can be used to describe the spatial distribution, at a later epoch, of Press–Schechter clumps identified at some earlier epoch. Section 4.4 relates this description of the merging of Press–Schechter clumps to the compound cluster model of Section 3.2. Section 4.5 develops a detailed model for the development, on all levels of the hierarchy, of hierarchical clustering.

Section 5 compares many of the analytic results of the preceding sections with N-body simulations of gravitational clustering in a system of identical particles that initially have a Poisson spatial distribution, and have no initial velocities. The results show very good agreement with the analytic, Press–Schechter predictions: the Borel cluster centres defined at a given epoch initially have a Poisson spatial distribution, and the subsequent clustering of these cluster centres is well approximated by equation (1), consistent with the theoretical results obtained in Sections 2, 3, and 4. The single mass simulations used in Sections 5.1 and 5.2 do not have sufficient resolution to allow quantitative tests of the analytic predictions of the development of hierarchical clustering that are derived in Section 4. Such tests will be reserved for future work, although the results of Lacey & Cole (1994) strongly suggest that the agreement with merger rates measured in N-body simulations will be substantial.

The study of compound Poisson cluster models (Section 3.2, in particular), the approximate hierarchical clustering model developed in Section 3.4, and the detailed merger history model of Sections 4.3 and 4.5 all provide new insight that, in Section 5.3, is used to clarify the results of N-body simulations of gravitational clustering in which particles are not identical but have a range of masses. Section 5.3 argues that the multimass simulations can be used to test the accuracy of the expressions that describe the probability a clump has a given number of progenitors (equations 52–60). These multimass simulations strongly suggest that the model of Section 4.5 is, substantially, correct, so that the merger probabilities derived in Section 4.3 are also, substantially, correct. Section 6 summarizes the results and points the way towards future work.

2 NON-LINEAR THEORY AND HIERARCHICAL CLUSTERING

This section shows that equation (1) can be derived from a consideration of the excursion set mass spectrum of a Poisson distribution. This derivation of equation (1) is obtained without any explicit consideration of thermodynamics.

2.1 Excursion set mass functions for a Poisson distribution

Following the work of Epstein (1983) this subsection derives the Borel distribution from a consideration of the spectrum of mass fluctuations for a Poisson point distribution. This model, or description, of non-linear gravitational clustering is similar to that of the theory of Press & Schechter (1974) which has recently been extended by Bond et al. (1991). (See this latter work for a clear and detailed account of the Press–Schechter approach.)

Consider a Poisson distribution of identical particles with density $\bar{n}$, and let $f(k,\Delta)$ denote the probability that a given particle is at the centre of a spherical cluster of exactly k particles, and that the cluster is denser than the background by a factor Δ. That is, $f(k,\Delta)$ denotes the probability that the given particle is at the centre of a sphere of volume

$$V_k = \frac{k}{\bar{n}(1+\Delta)}, \tag{3}$$

and that all volumes greater than V_k are less dense than V_k itself. In other words, if $N(V)$ denotes the number of particles in the volume V centred on the chosen particle, then $f(k,\Delta)$ denotes the probability that $N(V_k) = k$ and that $N(V_{k+j}) < (k+j)$. Since the distribution is Poisson, these two probabilities are independent so that

$$f(k,\Delta) = f^{\mathrm{I}}(k,\Delta)\, f^{\mathrm{E}}(k,\Delta), \tag{4}$$

where the first factor (superscript I) denotes the probability that there are exactly k objects in the sphere V_k that is centred on the chosen particle (i.e., that $N(V_k) = k$), and the second term (superscript E) denotes the probability that V_k is the largest sphere centred on the chosen particle with the required overdensity Δ (i.e., there is no larger concentric sphere of volume V_{k+j} such that $N(V_{k+j}) = k+j$). Note that for a Poisson distribution all particles are uncorrelated so that $f^{\mathrm{E}}(k,\Delta)$ is independent of k, so it may be denoted $f^{\mathrm{E}}(\Delta)$.

Downloaded from https://academic.oup.com/mnras/article/276/3/796/1034602 by U.S. Department of Justice user on 17 August 2022

© Royal Astronomical Society • Provided by the NASA Astrophysics Data System

1995MNRAS.276..796S

From equation (3), the mean number of objects in V_k is

$$\bar{n}_k \equiv \bar{n} V_k = k/(1+\Delta), \tag{5}$$

and, since it is known that there is already one particle in the centre and that the other $(k-1)$ are uncorrelated (because the distribution is Poisson),

$$f^{\mathrm{I}}(k,\Delta) = \frac{\bar{n}_k^{k-1} \mathrm{e}^{-\bar{n}_k}}{(k-1)!}. \tag{6}$$

To obtain $f^{\mathrm{E}}(\Delta)$, first consider $1-f^{\mathrm{E}}(\Delta)$ which is the probability that there is at least one concentric sphere of volume V_{k+j} such that $N(V_{k+j}) = (k+j)$. Equation (3) shows that $V_{k+j} - V_k = V_j$ so that the requirement that $N(V_{k+j}) = (k+j)$ is equivalent to requiring that $N(V_j) = j$. So, for a Poisson distribution, $1-f^{\mathrm{E}}(\Delta)$ represents the sum over the probabilities that a given shell of volume V_j is the largest shell to have an overdensity as great as Δ. This means that

$$1-f^{\mathrm{E}}(\Delta) = \sum_{j=1}^{\infty} \frac{\bar{n}_j^j \mathrm{e}^{-\bar{n}_j}}{j!} f^{\mathrm{E}}(\Delta) = f^{\mathrm{E}}(\Delta) \sum_{j=1}^{\infty} \frac{\bar{n}_j^j \mathrm{e}^{-\bar{n}_j}}{j!}. \tag{7}$$

A second expression for $f^{\mathrm{E}}(\Delta)$ is obtained by noting that since $N(V_k)$ is never less than unity, and since it is almost certain that, as the radius of the sphere becomes very large, the density in that sphere tends to the average density $\bar{n}$,

$$\sum_{k=1}^{\infty} f(k,\Delta) = 1. \tag{8}$$

This normalization, with equations (5) for $\bar{n}_k$ and (6) for $f^{\mathrm{I}}(k,\Delta)$, when combined with equation (7) shows that

$$f^{\mathrm{E}}(\Delta) = \Delta/(1+\Delta), \tag{9}$$

so that

$$f(k,\Delta) = \frac{\Delta}{(1+\Delta)} \frac{\bar{n}_k^{k-1} \mathrm{e}^{-\bar{n}_k}}{(k-1)!} = \frac{\Delta}{(1+\Delta)} \left(\frac{k}{1+\Delta}\right)^{k-1} \frac{\mathrm{e}^{-k/(1+\Delta)}}{(k-1)!}. \tag{10}$$

This expression for the probability that a given particle of a Poisson distribution is at the centre of a cluster of size k was first obtained by Epstein (1983). It is the discrete analogue of the multiplicity function (including the ad hoc factor of two) obtained by Press & Schechter (1974) for non-linear clustering from an initially Gaussian field. The Press–Schechter result is obtained in the limit of large k and small Δ; with the use of Stirling's approximation for the factorial in equation (10),

$$f(k,\Delta) \rightarrow \frac{\Delta}{(1+\Delta)} \left(\frac{k}{1+\Delta}\right)^{k-1} \frac{\mathrm{e}^{-k/(1+\Delta)}k}{\sqrt{2\pi k}\, \mathrm{e}^{-k} k^k} \simeq \frac{\Delta}{\sqrt{2\pi k}} \exp\left(-\frac{k\Delta^2}{2}\right). \tag{11}$$

It is possible to provide an alternative derivation of equation (10). Let $p(V_c,\Delta)$ denote the probability that a given particle is at the centre of a sphere of size V_c, and that the sphere is overdense by the factor Δ or more. As before, let $\bar{n}V_c \equiv c/(1+\Delta)$. Thus, $p(V_c,\Delta)$ is the probability that a sphere of volume V_c contains j particles when it is known that there is certainly one particle in the centre of V_c, summed over all $j \geqslant c$. Since the underlying distribution is Poisson, and since there is certainly one particle at the centre of the sphere, this means that

$$p(V_c,\Delta) = \sum_{j=c}^{\infty} \frac{(\bar{n}V_c)^{j-1} \mathrm{e}^{-\bar{n}V_c}}{(j-1)!} = \sum_{j=c}^{\infty} \left(\frac{c}{1+\Delta}\right)^{j-1} \frac{\mathrm{e}^{-c/(1+\Delta)}}{(j-1)!}. \tag{12}$$

Now, there are at least two other ways of expressing this probability. Since, for a Poisson distribution, different volumes are independent, $p(V_c,\Delta)$ can be expressed by a double sum:

$$p(V_c,\Delta) = \sum_{k=c}^{\infty} \sum_{N=c}^{k} \begin{pmatrix} \text{probability} \\ N \text{ particles} \\ \text{within } V_c \end{pmatrix} \times \begin{pmatrix} \text{probability} \\ (k-N) \text{ particles} \\ \text{in } V_k - V_c \end{pmatrix} \times f^{\mathrm{E}}(k,\Delta), \tag{13}$$

where $f^{\mathrm{E}}(k,\Delta)$ is the probability that V_k is the largest sphere centred on the chosen particle that has the required overdensity Δ. For a Poisson distribution, $f^{\mathrm{E}}(k,\Delta)$ is given by equation (9). Thus,

$$\begin{aligned} p(V_c,\Delta) &= \sum_{k=c}^{\infty} \sum_{N=c}^{k} \frac{(\bar{n}V_c)^{N-1}}{(N-1)!} \mathrm{e}^{-\bar{n}V_c} \frac{(\bar{n}V_k - \bar{n}V_c)^{k-N}}{(k-N)!} \mathrm{e}^{-\bar{n}V_k - \bar{n}V_c} \left(\frac{\Delta}{1+\Delta}\right) \\ &= \sum_{k=c}^{\infty} \left(\frac{\Delta}{1+\Delta}\right) \sum_{N=c}^{k} \left(\frac{c}{1+\Delta}\right)^{N-1} \left(\frac{k-c}{1+\Delta}\right)^{k-N} \frac{\mathrm{e}^{-k/(1+\Delta)}}{(N-1)!(k-N)!} \\ &= \sum_{k=c}^{\infty} \left(\frac{\Delta}{1+\Delta}\right) \left(\frac{k}{1+\Delta}\right)^{k-1} \frac{\mathrm{e}^{-k/(1+\Delta)}}{(k-1)!} \sum_{N=c}^{k} \binom{k-1}{N-1} \left(\frac{c}{k}\right)^{N-1} \left(\frac{k-c}{k}\right)^{k-N}. \end{aligned} \tag{14}$$

© Royal Astronomical Society • Provided by the NASA Astrophysics Data System

Downloaded from https://academic.oup.com/mnras/article/276/3/796/1034602 by U.S. Department of Justice user on 17 August 2022

1995MNRAS.276..796S

The equality of equations (12) and (14) can be shown by using relations similar to the identities

$$e^{ax} = \sum_{n=0}^{\infty} \frac{(xe^{-x})^n}{n!}\, a\,(a+n)^{n-1} \quad \text{and} \tag{15}$$

$$\frac{e^{ax}}{1-x} = \sum_{n=0}^{\infty} \frac{(xe^{-x})^n}{n!}\, (a+n)^n, \tag{16}$$

which follow from Lagrange's theorem on the inversion of series (e.g. Riordan 1979, p. 147), and other identities that are associated with Consul's (1989) generalized Poisson distribution

$$P(N) = \frac{\theta\,(\theta+N\lambda)^{N-1}}{N!}\, e^{-\theta-N\lambda}, \qquad \theta>0, \quad \lambda<1. \tag{17}$$

The central moments, $\mu_i \equiv \sum (N-\mu_1)^i P(N)$, of this distribution are particularly useful. The first two central moments are $\mu_1 = \theta/(1-\lambda)$ and $\mu_2 = \theta/(1-\lambda)^3$ (e.g. Consul 1989, p. 50).

However, it is also true that

$$p(V_c,\Delta) = \sum_{k=c}^{\infty} \begin{pmatrix} \text{probability that the largest} \\ \text{sphere centred on the chosen} \\ \text{particle that is overdense by} \\ \Delta \text{ or more has size } V_k \end{pmatrix} \times \begin{pmatrix} \text{probability that the sphere} \\ V_c < V_k \text{ centred on the same} \\ \text{particle is also overdense by} \\ \Delta \text{ or more} \end{pmatrix}. \tag{18}$$

By definition, the first term on the right of equation (18) is the same as $f(k,\Delta)$. The second term on the right is the probability that there are between c and k particles in the volume $V_c < V_k$, given that there are k particles in the sphere V_k, and that all spheres concentric to, but larger than, V_k are less dense than $\bar{n}(1+\Delta)$. Since the underlying distribution is Poisson, the probability that there are between c and k particles in the sphere $V_c < V_k$, and $k-c$ particles in the shell $V_k - V_c$, is independent of the fact that all (concentric) spheres $V > V_k$ are less dense than $\bar{n}(1+\Delta)$. Therefore, the probability that the sphere V_c is overdense by Δ or more, given that there are k particles in V_k, is obtained by summing the probability that V_c has j particles and $V_k - V_c$ has $k-j$ particles, over all j that satisfy $c \leqslant j \leqslant k$. The Poisson assumption means that this probability may be calculated by using the Binomial distribution. However, recall that it is known that there is certainly one particle at the centre of the (concentric) spheres V_c and V_k. Therefore, this probability is identical to the expression given by the second sum on the last line of equation (14). Since equations (14) and (18) are equivalent descriptions of the same probability $p(V_c,\Delta)$, it must be that $f(k,\Delta)$ is given by the first set of terms on the right of the last line of equation (14). Comparison of equations (10) and (14) shows that these two expressions for $f(k,\Delta)$ are the same. Thus, relating $f(k,\Delta)$ to $p(V_c,\Delta)$ provides a way to calculate $f(k,\Delta)$ that differs from Epstein's (1983) original derivation.

2.2 Relation to equation (1)

When the number density of particles is $\bar{n}$, then $\bar{n}(1-b)\,\eta(N,b)$ with $\eta(N,b)$ given by equation (2) gives an expression for the number density of (Poisson distributed) clusters of size N for a distribution described by equation (1). Multiplying $\bar{n}(1-b)\,\eta(N,b)$ by N, the number of particles in a cluster of size N, and dividing by the number density of particles, $\bar{n}$, gives the probability that a particle is a member of an N-sized cluster. Setting

$$b = 1/(1+\Delta) \tag{19}$$

shows that the Borel cluster decomposition of equation (1) is essentially the same as the cluster multiplicity function provided by equation (10). Indeed, equation (19) yields a very suggestive interpretation for the b parameter of the Borel distribution. Namely, since $b = 1/(1+\Delta) = \bar{n}/\bar{n}(1+\Delta)$, it is the ratio of the average density $\bar{n}$ to the threshold density $\bar{n}(1+\Delta)$.

Having shown that the excursion set description of the Poisson distribution can be related to the Borel distribution, and knowing that the Borel distribution is closely related to the counts-in-cells distribution of equation (1), we can ask if this excursion set description can be related to equation (1) also. Recall that, in the Borel decomposition of equation (1), the Borel clusters have a Poisson spatial distribution. Section 3 of this paper will show that these Press–Schechter clumps are also expected to have a Poisson spatial distribution. However, if these Press–Schechter clumps have a Poisson spatial distribution, then equation (1) will describe the distribution of counts-in-cells for this Poisson Press–Schechter distribution of clumps. In other words, this excursion set, Press–Schechter treatment of the Poisson distribution is, in effect, a derivation of equation (1) that is effected without any explicit consideration of thermodynamic fluctuation theory. Therefore, equation (1) will be referred to as the Poisson Press–Schechter distribution (PPSD), hereafter.

Insofar as the Press–Schechter theory describes clustering in a density field that is initially Gaussian, the PPSD functional form should describe clustering in a discrete distribution that is initially Poisson. Thus, this derivation of the Borel distribution (i.e., essentially, equation 10) shows why the PPSD functional form fits the N-body simulations of gravitational clustering from an initially Poisson distribution so well. It also shows that the PPSD functional form may be expected to describe gravitational

Downloaded from https://academic.oup.com/mnras/article/276/3/796/1034602 by U.S. Department of Justice user on 17 August 2022

© Royal Astronomical Society • Provided by the NASA Astrophysics Data System

1995MNRAS.276..796S

clustering from Poisson initial conditions regardless of whether or not the thermodynamic theory developed by Saslaw & Hamilton (1984) really applies.

This result also clarifies some results regarding N-body simulations of gravitational clustering from initial conditions that are significantly different from Poisson. Saslaw (1985) and Suto et al. (1990) note that equation (1) fits counts-in-cells distribution functions for simulations of clustering from Poisson initial conditions, but is not so accurate when the initial conditions differ from Poisson. In general, the Press–Schechter multiplicity functions depend on the initial conditions (e.g. Press & Schechter 1974; Bond et al. 1991). Therefore, this subsection shows explicitly that the lack of agreement between the PPSD functional form and simulations of clustering from arbitrary non-Poisson initial distributions is largely due to the intimate connection between the Borel and the Poisson distributions.

Downloaded from https://academic.oup.com/mnras/article/276/3/796/1034602 by U.S. Department of Justice user on 17 August 2022

2.3 Evolution of the overdensity threshold

The excursion set mass functions calculated in Section 2.1 are obtained without any reference to the role played by gravity, other than that gravity causes (spherical) density enhancements to collapse. In the usual Press–Schechter analysis, gravity is incorporated into the excursion set description by using the dynamics of spherical gravitational collapse to compute the time evolution of the overdensity threshold, Δ, that is required for collapse (e.g. Press & Schechter 1974; Bond et al. 1991). In this subsection, gravity is included by calculating the gravitational evolution of the variance (on the large scales where this evolution is still linear, and so calculable), and then using this evolution to describe the evolution of the overdensity threshold required for gravitational collapse.

Zhan (1989), using linear perturbation theory (e.g. Peebles 1980, section 70), considers the gravitational evolution of an initially cold, Poisson distribution of particles. For such a system, he calculates the evolution of the variance of the density distribution on the very large scales where linear theory applies. Zhan uses the standard linearized equations of motion for an ideal fluid to calculate the evolution of the long-wavelength modes of density contrast $\delta_{\boldsymbol{k}}(t)$, which, in linear theory, are easily related to the variance of the matter distribution. For an initially cold Poisson distribution these long-wavelength modes are independent of k (e.g. Peebles 1980, section 70). For such a system the variance is

$$\left\langle\left(\frac{\delta M}{M}\right)^2\right\rangle = \frac{V_{\mathrm{u}}}{(2\pi)^3}\int_0^{\infty}\left|\delta_{\boldsymbol{k}}(t)\right|^2\, W(kr)\,\mathrm{d}^3k \propto V_{\mathrm{u}}\, r^{-3}\, D^2(t), \tag{20}$$

where V_{u} is a periodic volume that contains exactly N_t particles, so that $N_t = \bar{n}V_{\mathrm{u}}$, $W(kr)$ is the window function that describes a spherical top-hat volume (e.g. Peebles 1980), and $D^2(t) \propto \langle|\delta_{\boldsymbol{k}}|^2\rangle$. The final expression follows because the long-wavelength modes are independent of k.

If the matter distribution is described by the PPSD on all scales, then on any scale the variance is

$$\frac{1}{\bar{N}^2}\left\langle(N-\bar{N})^2\right\rangle = \frac{1}{\bar{N}\left(1-b(t)\right)^2} \tag{21}$$

(e.g. Saslaw & Hamilton 1984; Saslaw 1989). Zhan argues that on scales where linear theory applies it is valid to equate equations (20) and (21), so that

$$b(t) = \frac{D(t)-1}{D(t)}, \tag{22}$$

with $D(t_i) = 1$ so that the initial value of $b(t_i) = 0$, which is consistent with the requirement that the initial distribution be Poisson. When $\Omega_0 = 1$, then

$$\frac{1}{1-b(t)} = D(t) = \frac{3}{5}\frac{a(t)}{a_i} + \frac{2}{5}\left(\frac{a(t)}{a_i}\right)^{-3/2}, \tag{23}$$

with $a(t) \propto t^{2/3}$. When $\Omega_0 \neq 1$, then the evolution of $D(t)$, and so $b(t)$, is obtained by numerically integrating

$$\frac{\mathrm{d}^2 D(x)}{\mathrm{d}x^2} + \frac{3 \pm 4x}{2x\,(1\pm x)}\,\frac{\mathrm{d}\,D(x)}{\mathrm{d}x} - \frac{3\,D(x)}{2x^2\,(1\pm x)} = 0, \tag{24}$$

with $x = |1-\Omega|/\Omega$, and where the $\pm$ cases correspond to open and closed cosmologies (Zhan 1989).

Using equation (24) for the linear theory evolution of the variance, and so of b, and equation (19) for the relation between the overdensity threshold, Δ, and b, shows that Δ decreases as the universe expands so that, in cosmologies with $\Omega_0 = 1$,

$$\Delta = \left(\frac{1-b}{b}\right) = \left[\frac{3a}{5a_i} + \frac{2}{5}\left(\frac{a}{a_i}\right)^{-3/2} - 1\right]^{-1}, \tag{25}$$

where a/a_i is the expansion factor of the simulations (and is denoted R in Fig. 6). When a/a_i is large, this evolution differs only slightly from the usual (e.g. Bond et al. 1991) expression, $\Delta = 1.69\,(1+z)$, where z is the redshift, for the evolution of Δ for an

© Royal Astronomical Society • Provided by the NASA Astrophysics Data System

1995MNRAS.276..796S

initially Gaussian random field. Notice that this evolution reproduces the standard expression even though it is independent of the details of the assumed spherical collapse. This close agreement between the standard approach and the one used in this section is most probably due to the fact that most high peaks of a three-dimensional Gaussian density field are, indeed, spherical (e.g. Adler 1981; Bardeen et al. 1986; Bernardeau 1994).

3 MASS FUNCTIONS FOR COMPOUND POISSON CLUSTER MODELS

It is relatively straightforward to generalize Epstein's result to the compound Poisson cluster models described by Sheth & Saslaw (1994). This section presents a generalization of the results of Section 2.1. It treats the case of generic compound Poisson cluster models and shows that the excursion sets of a PPSD, with the appropriate rescaling of variables, are similar to those for a Poisson distribution. In contrast to the expression for the excursion sets of a PPSD in the limit of very massive clumps derived by Lucchin & Matarrese (1988), the analysis here is exact.

3.1 Generic compound Poisson distributions

Define V_k and $\bar{n}_k$ as before (equations 3 and 5), and again, since the distribution of point clusters is Poisson, $f_{\rm CP}(k,\Delta)$ separates into two terms. The first term is

$$f^{\rm I}_{\rm CP}(k,\Delta) = \sum_{m=1}^{k}\left(\begin{array}{c}\text{probability particle}\\ \text{is in cluster with}\\ m \text{ particles}\end{array}\right)\times\left(\begin{array}{c}\text{probability there are}\\ (k-m)\text{ other}\\ \text{particles in } V_k\end{array}\right)$$

$$= \sum_{m=1}^{k}\frac{\bar{n}_{\rm clus}}{\bar{n}}\, m\,\eta(m)\,P_{\rm CP}(k-m,\bar{n}V_k), \tag{26}$$

where $\bar{n}_{\rm clus}/\bar{n}$ is the ratio of the density of cluster centres to that of particles, $\eta(m)$ denotes the probability that a randomly placed, point-shaped cluster has exactly m particles, and $P_{\rm CP}(k-m,\bar{n}V_k)$ denotes the probability that a randomly placed cell, having a volume such that the mean number of particles is $\bar{n}V_k$, has exactly $(k-m)$ particles. For a Poisson distribution $\eta(1)=1$ and $\eta(m)=0$ when $m\neq 1$ so that this, with the Poisson distribution for $P_{\rm CP}(k-m,\bar{n}V_k)$, shows that equation (26) reduces to equation (6) when the distribution is Poisson. Similarly,

$$1-f^{\rm E}_{\rm CP}(\Delta) = \sum_{j=1}^{\infty}\left(\begin{array}{c}\text{probability there are}\\ j\text{ particles in } V_j\end{array}\right)\times f^{\rm E}_{\rm CP}(\Delta)$$

$$= f^{\rm E}_{\rm CP}(\Delta)\sum_{j=1}^{\infty}P_{\rm CP}(j,\bar{n}V_j), \tag{27}$$

and, again, requiring that the sum of $f_{\rm CP}(k,\Delta)$ over k equal unity provides a second expression for $f^{\rm E}_{\rm CP}(\Delta)$. These two equations can be solved for $f^{\rm E}_{\rm CP}(\Delta)$ and so for $f_{\rm CP}(k,\Delta)$.

3.2 A simple scaling solution

For the general compound Poisson distribution the solution to the system of equations presented in the previous subsection is quite complicated. However, the special case when $P_{\rm CP}(j,\bar{n}V_j)$ is a PPSD (i.e., it is given by equation 1) exhibits a remarkable scaling. In this case

$$\begin{aligned} f^{\rm E}_{\rm CP}(\Delta) &= \left[1+\sum_{j=1}^{\infty}P_{\rm CP}(j,\bar{n}V_j)\right]^{-1}\\ &= \left[1+\sum_{j=1}^{\infty}\frac{\bar{n}_j(1-b)}{j!}\left(\bar{n}_j(1-b)+jb\right)^{j-1}\mathrm{e}^{-\bar{n}_j(1-b)-jb}\right]^{-1}\\ &= \left[1+\sum_{j=1}^{\infty}\frac{j^j}{j!}\left(\frac{1-b}{1+\Delta}\right)\left(\frac{1+\Delta b}{1+\Delta}\right)^{j-1}\mathrm{e}^{-j(1+\Delta b)/(1+\Delta)}\right]^{-1}\\ &= \left[1+\left(\frac{1-b}{1+\Delta}\right)\frac{(1+\Delta)}{\Delta(1-b)}\right]^{-1}\\ &= \frac{\Delta}{(1+\Delta)}, \end{aligned} \tag{28}$$

Downloaded from https://academic.oup.com/mnras/article/276/3/796/1034602 by U.S. Department of Justice user on 17 August 2022

© Royal Astronomical Society • Provided by the NASA Astrophysics Data System

1995MNRAS.276..796S

where the solution is facilitated by noticing that the sum over j is essentially the first moment of a Borel distribution with parameter, say, $B \equiv (1+\Delta b)/(1+\Delta)$, so that the first moment is $1/(1-B)$. Notice that $f^{\rm E}_{\rm CP}(\Delta)$ for a compound Poisson PPSD model is the same as for a Poisson distribution (compare equation 9). Similarly,

$$\begin{aligned} f^{\rm I}_{\rm CP}(k,\Delta) &= \sum_{m=1}^{k} \frac{\bar n_{\rm clus}}{\bar n}\, m\,\eta(m)\, P_{\rm CP}(k-m,\bar n V_k) \\ &= \sum_{m=1}^{k} m(1-b)\,\frac{(mb)^{m-1}}{m!}\,{\rm e}^{-mb}\,\frac{\bar n_k(1-b)}{(k-m)!}\left(\bar n_k(1-b)+(k-m)b\right)^{k-m-1}{\rm e}^{-\bar n_k(1-b)-(k-m)b} \\ &= (1-b)\,\frac{(kB)^{k-1}\,{\rm e}^{-kB}}{(k-1)!}\left(\frac{1-b}{1+\Delta}\right)\sum_{m=1}^{k}\binom{k}{m}\, m\,\frac{(mb)^{m-1}}{(kB)^{k-1}}\,(kB-mb)^{k-m-1} \\ &= (1-b)\,\frac{(kB)^{k-1}\,{\rm e}^{-kB}}{(k-1)!}\left(\frac{1-b}{1+\Delta}\right)\frac{1}{(B-b)} \\ &= (1-b)\,\frac{(kB)^{k-1}\,{\rm e}^{-kB}}{(k-1)!}, \end{aligned} \tag{29}$$

where $B \equiv (1+\Delta b)/(1+\Delta)$ as before, and Abel's (1826) generalization of the Binomial identity,

$$(x+y)^k = \sum_{m=0}^{k}\binom{k}{m}\, x[x-mz]^{m-1}[y+mz]^{k-m}, \tag{30}$$

was used to simplify the analysis considerably. This, with equations (4) and (28), shows that

$$f_{\rm CP}(k,\Delta) = \frac{\Delta(1-b)}{(1+\Delta)}\,\frac{(kB)^{k-1}\,{\rm e}^{-kB}}{(k-1)!} = (1-B)\,\frac{(kB)^{k-1}\,{\rm e}^{-kB}}{(k-1)!}, \tag{31}$$

which has exactly the same form as equation (10), except that b (which for equation 10 was equal to $1/[1+\Delta]$) is replaced by B. This shows that the excursion set multiplicity function of a compound Poisson PPSD model has the same functional form as that for a Poisson distribution. Whereas the Lucchin & Matarrese (1988) solution for the multiplicity function of a PPSD only applies in the very massive clump limit, and only when $b \to 1$, equation (31) is exact for arbitrary masses, and for all permitted values of $0 \leqslant b \leqslant B \leqslant 1$.

Finally, note that this scaling solution strongly suggests that the spatial distribution of the Press–Schechter clumps derived in Section 2.1 is, indeed, Poisson. Thus, this scaling solution justifies the assumption, implicit in the calculation of Section 2.3, that the counts-in-cells distribution function that corresponds to the Press–Schechter description of clustering from an initially Poisson distribution is a PPSD.

3.3 The Negative Binomial

In their consideration of multiplicity functions of non-Gaussian distributions, Lucchin & Matarrese (1988) also calculate the large-mass multiplicity function for a Negative Binomial distribution. Since a Negative Binomial distribution is a Poisson distribution compounded with a Logarithmic distribution (e.g. Moran 1984), the results of Section 3.1 can also be used to calculate the exact excursion set mass functions of Negative Binomial distributions, for clumps of arbitrary mass.

The generating function of the Logarithmic distribution is

$$g(t) = -\alpha\,\log(1-qt) = \alpha\sum_{i=1}^{\infty}\frac{q^i t^i}{i}, \tag{32}$$

where $\alpha = -1/\log(1-q)$, and $0 < q < 1$. So, the generating function of the Negative Binomial distribution for counts in cells of size V is $H(t) = {\rm e}^{\lambda[g(t)-1]}$, where $\lambda = -[\bar n V(1-q)\log(1-q)]/q$. The corresponding counts-in-cells distribution is

$$P_{\rm NB}(N,\bar n V) = \frac{{\rm e}^{-\lambda}}{N!}\prod_{i=0}^{N-1}\left(\bar n V(1-q)+iq\right). \tag{33}$$

The excursion set mass functions are $f_{\rm NB}(k,\Delta) = f^{\rm E}_{\rm NB}(\Delta) f^{\rm I}_{\rm NB}(k,\Delta)$, where

$$f^{\rm E}_{\rm NB}(\Delta) = \left[1+\sum_{j=1}^{\infty}P_{\rm NB}\left(j,\frac{\bar n j}{\bar n(1+\Delta)}\right)\right]^{-1} = \left[1+\sum_{j=1}^{\infty}q^j(1-q)^{\frac{j(1-q)}{(1+\Delta)q}}\binom{\frac{j(1-q)}{(1+\Delta)q}+j-1}{j}\right]^{-1}, \tag{34}$$

Downloaded from https://academic.oup.com/mnras/article/276/3/796/1034602 by U.S. Department of Justice user on 17 August 2022

© Royal Astronomical Society • Provided by the NASA Astrophysics Data System

1995MNRAS.276..796S

and

$$f^{\mathrm{I}}_{\mathrm{NB}}(k,\Delta)=\sum_{m=1}^{k}\left(\frac{1-q}{q}\right)(1-q)^{\frac{k(1-q)}{(1+\Delta)q}}\frac{q^k}{(k-m)!}\prod_{i=0}^{k-m-1}\left(\frac{k(1-q)}{(1+\Delta)q}+i\right). \tag{35}$$

Since $f^{\mathrm{E}}_{\mathrm{NB}}(\Delta)$ is independent of k,

$$f_{\mathrm{NB}}(k,\Delta)\propto q^{k-1}(1-q)^{Ak-1}\binom{Ak+k-1}{k-1}, \tag{36}$$

where $A=q^{-1}(1-q)/(1+\Delta)$, and the Binomial identity has been used to simplify the sum in equation (35). The Lucchin–Matarrese solution is obtained from this more general expression by using Stirling's approximation for the factorials, and taking the limit as $q\to 1$. Given the more interesting scaling solution found in the previous subsection for the PPSD, we will not consider the Negative Binomial distribution further in this paper.

3.4 Approximate model of hierarchical clustering

The scaling solution obtained in Section 3.2 suggests an interesting approximate model of the evolution of hierarchical clustering from an initially Poisson distribution. This model is developed below.

Consider a set of identical particles that initially have a Poisson spatial distribution. Also consider the set of Press–Schechter clusters identified at some epoch that corresponds to the overdensity threshold Δ_1. Equation (19) shows that the distribution of cluster members is described by the Borel distribution with the appropriate value of $b_1=1/(1+\Delta_1)$. Call these clusters the b_1-Borel clusters. When they are identified, these b_1-Borel clusters have a Poisson spatial distribution by assumption. That is, if all the b_1-Borel cluster centres are considered to be identical (i.e., no regard is taken of the number of particles associated with each b_1-Borel cluster), then the spatial distribution function of the resulting distribution of cluster centres is Poisson.

When the average density of particles is $\bar{n}$ the number density of the b_1-Borel clusters is $\bar{n}_{\mathrm{cen}}=\bar{n}(1-b_1)$. This means that the counts-in-cells distribution function of the b_1-Borel cluster centres is a PPSD with $b_{\mathrm{cen}}=0$ and with average number density $\bar{n}_{\mathrm{cen}}$. Of course, by definition, the counts-in-cells distribution of the particles themselves (as opposed to the b_1-Borel clusters) is the PPSD with parameters b_1 and $\bar{n}$. At some later time corresponding to a threshold $\Delta_2<\Delta_1$, the particles (and the b_1-Borel clusters that were identified at Δ_1) have had some time to cluster. Equation (10) shows that the counts-in-cells distribution of the particles at this later time, Δ_2, is a PPSD, with a value of $B=b_2$ that is larger than b_1 (the comoving density is still $\bar{n}$). What is the spatial distribution of the b_1-Borel clusters (that were defined at Δ_1) at this later epoch when the overdensity threshold is Δ_2?

To a crude first approximation, assume that the clustering of these b_1-Borel clusters occurs independently of the mass of each cluster. That is, assume that each b_1-Borel cluster has the mean number, $1/(1-b_1)$, of identical particles. This approximation is good for those values of b_1 for which the root mean square deviation around the mean value, $\sqrt{b_1/(1-b_1)^3}$, is somewhat less than, say, $\sqrt{1/(1-b_1)}$, the square root of the mean. So, provided $b_1\lesssim 0.35$ or so, the clustering of these b_1-Borel clusters (which had a Poisson spatial distribution at the epoch when they were identified, Δ_1) will, to a good approximation, be described by the approach that yielded equation (10). (Recall that Section 2.1 describes the Press–Schechter clustering of identical particles that initially have a Poisson distribution.) Thus, if b_1 is small, then the counts-in-cells distribution function of these b_1-Borel clusters at the later epoch corresponding to $\Delta_2<\Delta_1$ will also be a PPSD, with some value of b_{cen}, and with average number density $\bar{n}_{\mathrm{cen}}=\bar{n}(1-b_1)$.

The value of b_{cen} can be determined using the results of Section 3.2 as follows. Recall that the mean of a Borel distribution with parameter b is $1/(1-b)$. Thus, $1/(1-b_1)$ and $1/(1-b_2)$ are, respectively, the mean particle clump size at the epochs b_1 and b_2. Let $B=b_2$. Then $(1+\Delta)/\Delta=(1-b_1)/(1-b_2)$ in equations (28)–(31) can be interpreted as the mean size of clumps of b_1-Borel clusters. So, if the b_1-Borel clusters are themselves arranged (approximately) in Borel clumps with parameter b_{cen}, then Section 3.2 suggests that $(1-b_{\mathrm{cen}})=\Delta/(1+\Delta)=(1-b_2)/(1-b_1)$. In this approximation, therefore, when the counts-in-cells distribution function of the particles is a PPSD with parameters $B=b_2$ and $\bar{n}$, then the counts-in-cells distribution function of the b_1-Borel clusters that were identified when the particle PPSD was described by $b_1<B$ is also a PPSD but with parameters $b_{\mathrm{cen}}=(b_2-b_1)/(1-b_1)$ and $\bar{n}_{\mathrm{cen}}=\bar{n}(1-b_1)$.

This model of a Poisson distribution of super-cluster centres, in which the probability that a super-cluster has N associated b_1-Borel clusters is given by a Borel distribution with parameter b_{cen}, and the probability that a b_1-Borel cluster has M associated particles is given by a Borel distribution with parameter b_1, makes two approximations that must be checked by comparison with N-body simulations. When using the Press–Schechter approach (of Section 2.1) to compute the distribution of b_1-Borel clusters, the approximation that all the b_1-Borel clusters are identical is essentially the assumption that the clustering of the b_1-Borel clusters occurs without regard for the mass of each cluster. This assumption is almost certainly wrong, and the comparison with N-body simulations will quantify the importance of this effect.

Furthermore, it is possible to calculate the counts-in-cells distribution function of such a distribution of super-clusters. (The calculation is a straightforward, but tedious, exercise similar to the one shown by Sheth & Saslaw 1994.) The exact expression for

Downloaded from https://academic.oup.com/mnras/article/276/3/796/1034602 by U.S. Department of Justice user on 17 August 2022

© Royal Astronomical Society • Provided by the NASA Astrophysics Data System

1995MNRAS.276..796S

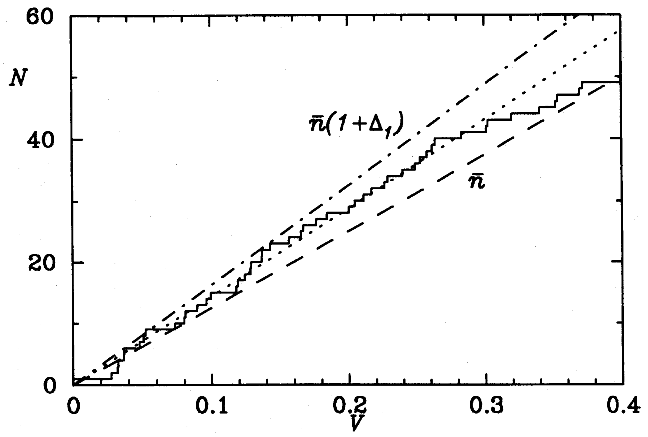

Figure 1. Example of the trajectory (solid line) traced by the number, N, of Poisson-distributed objects within a sphere of volume V, given that there is an object located at the centre of the sphere. The dashed line shows the average density, so it has slope $\bar{n}$; the dotted line shows the number required to give an overdensity of Δ_2; and the dot-dashed line, which has a slope of $\bar{n}(1+\Delta_1)$, shows the number required to give an overdensity of $\Delta_1 > \Delta_2$. As V becomes large, all trajectories fluctuate around the average density (dashed) curve.

the counts-in-cells distribution function of such a distribution of super-clusters is rather complicated. However, when b_1 and $b_{\rm cen}$ are both small (smaller than, say, ~ 0.35), then the exact distribution function is well approximated by the PPSD form. Since both b_1 and $b_{\rm cen}$ increase as the clustering evolves, this approximation, and so this particular model of super-clustering, is valid only at relatively early times.

Nevertheless, the approximate model developed here, for the evolution of hierarchical clustering from an initially Poisson distribution, which is suggested by the assumption that to lowest order the clustering of clusters proceeds independently of the masses of the clusters, and is valid at early times when b_1 and $b_{\rm cen}$ are both small, makes specific predictions that can be compared with N-body simulations of non-linear gravitational clustering. In particular, this model suggests that, once a set of Borel clusters has been identified at some epoch, the subsequent clustering of the Borel centres is hierarchical and stable; to a good approximation, rather than considering the details of the internal structure within each cluster, the clusters described by the Borel cluster decomposition may be replaced by point-shaped objects of the appropriate mass located at the centre-of-mass of the cluster. Then, to a first approximation (which neglects the differing masses of the clusters), the subsequent clustering of a given set of Borel clusters is also described by a PPSD. The compound Poisson excursion set mass function derived in Section 3.2 suggests that when the particle distribution is described by a PPSD with b_2, and the particles are arranged in b_1-Borel clusters, then the value, $b_{\rm cen}$, that describes the clustering of the b_1-Borel cluster centres is $(b_2 - b_1)/(1 - b_1)$.

4 MERGING AND HIERARCHICAL CLUSTERING

The previous section provided an approximate model for the development of hierarchical clustering from an initially Poisson distribution. The present section uses a different approach to obtain an alternative description of the growth of clustering that is also more precise.

4.1 The two-barrier problem

As argued by Bond et al. (1991), the excursion set formulation of the Press–Schechter theory shows clearly how to formulate and solve for a description of merging and hierarchical clustering. Essentially, the merging problem reduces to solving a two-barrier problem that is analogous to the one-barrier problem that was solved to obtain the multiplicity function at a given epoch (see also Lacey & Cole 1993). For an initially Poisson distribution the two-barrier problem is solved similarly to the one-barrier problem solved by Epstein and reviewed and extended in the previous sections. This section discusses exactly how the one-barrier problem was solved, and then makes the necessary adjustment for two barriers.

To solve the one-barrier problem, Epstein argued that he could break the probability $f(k,\Delta)$ up into an external term and an internal term. The internal term gives the probability that there are, say, k particles with the required overdensity. This internal term (equation 6) is obtained by summing over all possible trajectories that pass through the required overdensity point (see Fig. 1). For example, the term that gives three particles with the overdensity Δ is the sum over the trajectories $\{1,0,2\}$, $\{1,1,1\}$, $\{1,2,0\}$, $\{2,0,1\}$, $\{2,1,0\}$, and $\{3,0,0\}$, where $\{k,l,m\}$ means k particles in volume V_1, l particles in $(V_2 - V_1)$ and m particles in $(V_3 - V_2)$, and where V_j is defined in equation (3). (Since all trajectories start on a particle, there is always at least one particle in the smallest volume

Downloaded from https://academic.oup.com/mnras/article/276/3/796/1034602 by U.S. Department of Justice user on 17 August 2022

© Royal Astronomical Society • Provided by the NASA Astrophysics Data System

1995MNRAS.276..796S

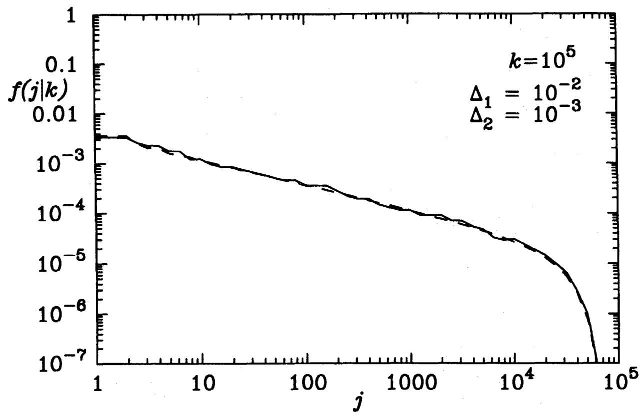

Figure 2. Conditional probability distribution (equation 40) for an initially Poisson distribution (solid line), and for a Gaussian distribution having a power spectrum with slope $n = 0$ (dashed line), for a representative choice of $k \gg 1$ and $1 \gg \Delta_1 \gg \Delta_2$.

V_1.) The result in equation (6) is obtained by simply adding up all the trajectories that meet the necessary criteria, and weighting each trajectory by the probability that it actually occurs. This is exactly what must be done to solve the two-barrier problem.

For example, to calculate the probability that a particle is in a clump of size k at overdensity Δ_1 given that it is in a clump (also) of size k but at overdensity Δ_2, with $\Delta_2 < \Delta_1$, first define $V_k^{[1]}$ and $V_k^{[2]}$ as in equation (3). Also, write

$$f(k, \Delta_1 | k, \Delta_2) = \frac{f(k, \Delta_1, k, \Delta_2)}{f(k, \Delta_2)}, \tag{37}$$

and solve for the quantity on the left. The denominator on the right, $f(k, \Delta_2)$, is given by an expression like equation (10). The numerator on the right is obtained by summing over all trajectories that have exactly k particles within volume $V_k^{[1]}$, exactly k particles within (the larger volume) $V_k^{[2]}$, and fewer than l particles in all (even larger) volumes V_l when $l > k$, and multiplying each trajectory by the requisite weighting factor. This means, for this example, that the shell $V_k^{[2]} - V_k^{[1]}$ is empty. Since the underlying distribution is Poisson, it is easy to calculate the probability that $V_k^{[2]} - V_k^{[1]}$ is void. Moreover, the probability that this shell is void is independent of the fact that there are exactly k particles within $V_k^{[1]}$, and also of the fact that there are fewer than l particles in all volumes V_l when $l > k$. So,

$$f(k, \Delta_1 | k, \Delta_2) = \frac{f^{\mathrm{I}}(k, \Delta_1)\, \mathrm{e}^{-\bar{n}\left(V_k^{[2]} - V_k^{[1]}\right)}\, f^{\mathrm{E}}(k, \Delta_2)}{f(k, \Delta_2)}, \tag{38}$$

where $f^{\mathrm{I}}(k, \Delta_1)$, $f^{\mathrm{E}}(k, \Delta_2)$, and $f(k, \Delta_2)$ come from equations (6), (7), and (10). This reduces to

$$f(k, \Delta_1 | k, \Delta_2) = \left(\frac{1 + \Delta_2}{1 + \Delta_1}\right)^{k-1}. \tag{39}$$

Similarly, to obtain $f(j, \Delta_1 | k, \Delta_2)$ with $j < k$ we must sum over all qualifying trajectories (and multiply by the appropriate weighting factors); these are all trajectories that have exactly j particles within $V_j^{[1]}$, fewer than l particles in $V_l^{[1]}$ where $j < l \leqslant k$, exactly k particles within $V_k^{[2]}$, and, thereafter, fewer than m particles in $V_m^{[2]}$ for all $m > k$.

For example, when $j = k - 1$ the qualifying trajectories are all those that have $k - 1$ particles within $V_{k-1}^{[1]}$, zero particles in the shell $V_k^{[1]} - V_{k-1}^{[1]}$ and one particle in the shell $V_k^{[2]} - V_k^{[1]}$. The generalization to the case when $j = k - m$ is straightforward, though it involves complicated combinatorics. The general result is

$$f(j, \Delta_1 | k, \Delta_2) = \binom{k}{j} \frac{j^j}{k^k} \left(\frac{1 + \Delta_2}{1 + \Delta_1}\right)^{k-1} \frac{k(\Delta_1 - \Delta_2)}{(1 + \Delta_2)} \left(\frac{k(\Delta_1 - \Delta_2)}{(1 + \Delta_2)} + m\right)^{m-1}, \tag{40}$$

where $\Delta_1 > \Delta_2$ and $k > j$ with $j = k - m$.

If this is normalized correctly, then

$$\sum_{j=1}^{k} f(j, \Delta_1 | k, \Delta_2) = \sum_{m=0}^{k-1} f(k - m, \Delta_1 | k, \Delta_2) = 1. \tag{41}$$

To show this, use the Abel identity (equation 30); it gives the required result when $x = k(\Delta_1 - \Delta_2)/(1 + \Delta_2)$, $y = k$, and $z = -1$. Using Stirling's approximation for the factorials, with $k \gg j \gg 1$ and $1 \gg \Delta_1 \gg \Delta_2$, shows that this result reduces to the appropriate result, for a Gaussian distribution that has a power spectrum with slope $n = 0$. The solid line in Fig. 2 shows the distribution of equation (40) for a representative choice of k, Δ_1, and Δ_2. The dashed line shows the relevant Gaussian result; since $k \gg 1$ and $\Delta_2 \ll \Delta \ll 1$, it is nearly indistinguishable from the Poisson result derived above.

Downloaded from https://academic.oup.com/mnras/article/276/3/796/1034602 by U.S. Department of Justice user on 17 August 2022

© Royal Astronomical Society • Provided by the NASA Astrophysics Data System

1995MNRAS.276..796S

The expression $f(j,\Delta_1|k,\Delta_2)$ denotes the fraction of the mass in a clump with k particles that was previously in a clump with j particles. Therefore, using equation (40), it is straightforward to calculate the mass fraction of a k-sized clump that was previously in clumps with sizes in the range between, say, $j_{\min}$ and $j_{\max}$, with $1 \leqslant j_{\min} < j_{\max} \leqslant k$; it is just the sum of all the $f(j,\Delta_1|k,\Delta_2)$ that have $j_{\min} < j < j_{\max}$. This property is used in the next subsection.

Finally, since

$$f(j,\Delta_1,k,\Delta_2) = f(k,\Delta_2)\,f(j,\Delta_1|k,\Delta_2) = f(j,\Delta_1)\,f(k,\Delta_2|j,\Delta_1)\,, \tag{42}$$

it is trivial to obtain an expression for the inverse statement, $f(k,\Delta_2|j,\Delta_1)$, from equations (10) and (40). Equations (41) and (42) show that summing $f(j,\Delta_1,k,\Delta_2) = f(k,\Delta_2)f(j,\Delta_1|k,\Delta_2)$ over all $1 \leqslant j \leqslant k$ equals $f(k,\Delta_2)$. Similarly, summing $f(j,\Delta_1,k,\Delta_2)$ over all $k \geqslant j$ should equal $f(j,\Delta_1)$. Writing Δ_1 in terms of b_1 and Δ_2 in terms of b_2 (equation 19) means that

$$\begin{aligned}
\sum_{k=j}^{\infty} f(j,\Delta_1,k,\Delta_2) &= \sum_{k=j}^{\infty} f(k,\Delta_2)\,f(j,\Delta_1|k,\Delta_2) \\
&= \sum_{k=j}^{\infty} \binom{k}{j} \frac{j^j}{k^{k-1}} \left(\frac{b_2-b_1}{b_1}\right) \left[k\left(\frac{b_2-b_1}{b_1}\right)+k-j\right]^{k-j-1} \left(\frac{b_1}{b_2}\right)^{k-1} (1-b_2)\frac{(kb_2)^{k-1}}{(k-1)!}\,\mathrm{e}^{-kb_2} \\
&= \frac{(b_1 j)^j}{j!}\left(\frac{b_2-b_1}{b_1}\right)(1-b_2)\sum_{N=0}^{\infty}\frac{(N+j)}{N!}\left[(N+j)\left(\frac{b_2-b_1}{b_1}\right)+N\right]^{N-1} b_1^{N-1}\mathrm{e}^{-Nb_2-jb_2} \\
&= \frac{(b_1 j)^{j-1}}{(j-1)!}(1-b_2)\sum_{N=0}^{\infty}\frac{(N+j)(b_2-b_1)}{N!}\Big[(N+j)(b_2-b_1)+Nb_1\Big]^{N-1}\mathrm{e}^{-j(b_2-b_1)-Nb_2-jb_1} \\
&= \frac{(b_1 j)^{j-1}}{(j-1)!}\mathrm{e}^{-jb_1}(1-b_2)\sum_{N=0}^{\infty}\frac{(N+j)}{j}\frac{j(b_2-b_1)}{N!}\Big[j(b_2-b_1)+Nb_2\Big]^{N-1}\mathrm{e}^{-j(b_2-b_1)-Nb_2} \\
&= \frac{(b_1 j)^{j-1}}{(j-1)!}\mathrm{e}^{-jb_1}(1-b_2)\left(\frac{j(b_2-b_1)}{j(1-b_2)}+1\right) = f(j,\Delta_1)
\end{aligned} \tag{43}$$

as required. The last line follows after recognizing Consul's distribution (equation 17) in the penultimate line in the expression above, and so substituting for the first moment of the generalized Poisson distribution (given in the text following equation 17). Bower (1991) gives the analogous relation for the Gaussian case. This demonstrates the self-consistency of the expressions for the merger probabilities that were derived in this subsection.

Following Lacey & Cole (1993), it is possible to determine a merger rate, $\mathrm{d}P(j \to k|\Delta)/\mathrm{d}\Delta$, by taking the limit as $\Delta_1 \to \Delta_2 = \Delta$ in $f(k,\Delta_2|j,\Delta_1)$:

$$\begin{aligned}
\frac{\mathrm{d}P(j\to k|\Delta)}{\mathrm{d}\Delta}\,\mathrm{d}\Delta &= \frac{k}{(k-j)!}\,\frac{\Delta_2}{\Delta_1}\,\frac{(\Delta_1-\Delta_2)}{(1+\Delta_2)^2}\left(\frac{k}{1+\Delta_2}-\frac{j}{1+\Delta_1}\right)^{k-j-1}\mathrm{e}^{-\frac{k}{1+\Delta_2}+\frac{j}{1+\Delta_1}} \\
&\to \frac{k}{\sqrt{2\pi}(k-j)^{3/2}}\,\frac{\mathrm{d}\Delta}{(1+\Delta)}\,\frac{\mathrm{e}^{k-j}\mathrm{e}^{-(k-j)/(1+\Delta)}}{(1+\Delta)^{k-j}} \\
&\to \frac{\mathrm{d}\Delta}{\sqrt{2\pi}}\left(\frac{k^2}{(k-j)}\right)^{3/2}\frac{\mathrm{e}^{-\Delta^2(k-j)/2}}{k^2}.
\end{aligned} \tag{44}$$

The second expression on the right follows from setting $\Delta_1 = \Delta_2 = \Delta$ and $\Delta_1 - \Delta_2 = \mathrm{d}\Delta$, and considering the limit when $k \gg j \gg 1$. Stirling's approximation for the factorials simplifies the expression considerably, and the final expression follows from assuming $\Delta \ll 1$. This last is similar to the expression derived by Lacey & Cole (1993). (In their notation $S_1 \propto 1/j, S_2 \propto 1/k$, and $\omega = \Delta$, since the relevant Gaussian corresponding to the Poisson is the white noise case. So equation 44 here reduces to their equation 2.17.)

4.2 Distribution of clump formation times

In what follows (and as a result of Section 2.3), the overdensity threshold Δ is treated as a pseudo-time variable, with Δ decreasing as the universe expands. The convention (consistent with Section 4.1) is to have $\Delta_1 > \Delta_2$.

From the results of the previous subsection, the number density of clumps of size j at the epoch corresponding to the threshold Δ_1 which have been incorporated into clumps of size k at the later epoch corresponding to $\Delta_2 > \Delta_1$ is $\bar{n}(1-b_1)\eta(j,b_1)f(k,\Delta_2|j,\Delta_1)$, where $\bar{n}$ denotes the number density of particles, $b_1 = 1/(1+\Delta_1)$ from equation (19), and $\eta(j,b_1)$ is the Borel distribution of equation (2). This means that the probability, $\eta(j,b_1|k,b_2)$, that a clump of size k at Δ_2 has a progenitor of size j at Δ_1 is given by dividing $\bar{n}(1-b_1)\eta(j,b_1)f(k,\Delta_2|j,\Delta_1)$ by $\bar{n}(1-b_2)\eta(k,b_2)$, the number density of clumps of size k at Δ_2. Thus,

$$\eta(j,b_1|k,b_2) = \binom{k}{j}\;f(j,\Delta_1|k,\Delta_2). \tag{45}$$

Downloaded from https://academic.oup.com/mnras/article/276/3/796/1034602 by U.S. Department of Justice user on 17 August 2022

© Royal Astronomical Society • Provided by the NASA Astrophysics Data System

1995MNRAS.276..796S

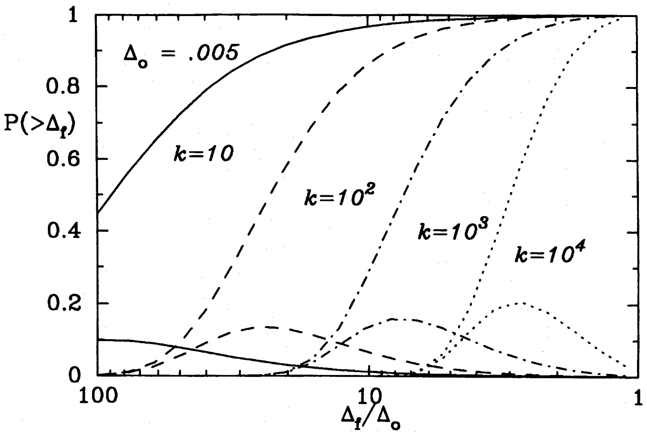

Figure 3. Cumulative (upper curves) and differential (lower curves) distributions of clump formation times, Δ_f, for clumps of size k that are identified at the epoch when the overdensity threshold is $\Delta_0 = 0.005$.

Whereas $f(j, \Delta_1|k, \Delta_2)$ denotes probability statements involving trajectories, $\eta(j, b_1|k, b_2)$ assumes that the trajectories involve actual physical clumps. A generalization of the Abel identity, namely,

$$\sum_{k=0}^{n} \binom{n}{k} (x+k)^{k-1}(y+n-k)^{n-k-1} = (x^{-1}+y^{-1})(x+y+n)^{n-1} \tag{46}$$

(equations 14 and 20 in section 1.5 of Riordan 1979), shows how to calculate the normalization of this distribution of clumps: $\sum_j \eta(j, b_1|k, b_2) = [b_1 + k(b_2 - b_1)]/b_2$, where the sum is over all $j \leqslant k$. As expected, this sum is greater than unity for all values of $0 < b_1 < b_2 < 1$ provided $k > 1$.

If a clump of size k is defined as having formed when one of its progenitor clumps is of size j, with the requirement that $k/2 < j \leqslant k$ (e.g. Lacey & Cole 1993), then the distribution of formation epochs, Δ_f, is easy to compute. It follows from the cumulative statement that gives the probability that a clump of size k at Δ_2 was formed at an epoch earlier than Δ_1:

$$P(\Delta_f > \Delta_1|k, \Delta_2) = P(j > k/2, \Delta_1|k, \Delta_2) = \sum_{j>k/2}^{k} \binom{k}{j} f(j, \Delta_1|k, \Delta_2). \tag{47}$$

Fig. 3 shows the distribution of clump formation times, Δ_f, as well as the cumulative distribution of equation (47) (denoted $P(>\Delta_f)$ in the figure), for a representative range of clump sizes k, and for a given value of the final epoch $\Delta_0 = 0.005$. As expected in this hierarchical clustering scenario, larger, more massive clumps form at later times than less massive clumps.

The trajectory probabilities satisfy another interesting identity that is not required by the consistency of the theory. Namely, the same generalization (equation 46) of Abel's generalization of the Binomial theorem that was used to derive equation (45) can be used to show that

$$\begin{aligned} \sum_{k_2=k_1}^{k_3} f(k_1, \Delta_1|k_2, \Delta_2)\, f(k_2, \Delta_2|k_3, \Delta_3) &= f(k_1, \Delta_1|k_3, \Delta_3), \\ \sum_{k_2=k_1}^{k_3} f(k_3, \Delta_3|k_2, \Delta_2)\, f(k_2, \Delta_2|k_1, \Delta_1) &= f(k_3, \Delta_3|k_1, \Delta_1), \end{aligned} \tag{48}$$

where $\Delta_1 \geqslant \Delta_2 \geqslant \Delta_3$, so that $k_1 \leqslant k_2 \leqslant k_3$. The second identity follows from the first after applying Bayes' theorem. These identities are the discrete analogues of those obtained by Bower (1991) and by White & Frenk (1991) for Gaussian random fields (although here we have explicitly shown that the sum must be taken only over those k_2 that have $k_1 \leqslant k_2 \leqslant k_3$). Using Bayes' theorem to relate the statement $f(k_1, k_2, k_3)$ (the notation here is obvious) to statements like $f(k_1|k_2)$ shows that equation (48) implies that $f(k_1|k_2, k_3) = f(k_1|k_2)$, provided $k_1 \leqslant k_2 \leqslant k_3$. That is, equation (48) is satisfied because the statements $f(j, \Delta_1|k, \Delta_2)$ are independent of what happened at times previous to Δ_1 and also of what will happen at times later than Δ_2 – the processes involved are Markov processes. This property will be useful in the next section.

4.3 The merger history tree

The previous subsections derived probability statements that, essentially, describe the probability that an object that is in a clump of size j when the overdensity threshold is Δ_1 is later in a clump of size k when the overdensity threshold is $\Delta_2 < \Delta_1$. However,

Downloaded from https://academic.oup.com/mnras/article/276/3/796/1034602 by U.S. Department of Justice user on 17 August 2022

© Royal Astronomical Society • Provided by the NASA Astrophysics Data System

1995MNRAS.276..796S

that description was obtained without consideration of the different ways in which the object of size j (when the threshold was Δ_1) could have merged with other objects to form the final object of size k (when the threshold is Δ_2). If the merging process is visualized as a tree (so trees having different numbers of branches, branch sizes and branching points describe different merger histories), a useful quantity is the probability that a particular tree structure, rather than any other, occurs. This subsection shows how to use the results of the previous subsection to solve for what is, essentially, the partition function for various tree structures.

Notice that the statements $f(j, \Delta_1|k, \Delta_2)$ are independent of what happened at times previous to Δ_1 and also of what will happen at times later than Δ_2. So, to solve for the entire merger history tree (i.e., for many $\Delta_1 < \Delta_2 < \ldots$) one need only know how to solve for the tree structure at any given two epochs, say, Δ_1 and Δ_2. Therefore, in what follows the later epoch, Δ_2, is referred to as the final epoch. Notice also that the statements $f(j, \Delta_1|k, \Delta_2)$ imply that it is possible to calculate the partition function for a tree with k particles without explicitly considering the partition function for trees with $l \neq k$ particles.

So, for any given pair of epochs Δ_1 and Δ_2, and for any tree whose final size (i.e., at the epoch Δ_2) is k, the problem is to calculate all possible tree configurations, and to assign to each configuration the probability that it actually occurs. The first step is to list all possible tree configurations, given that the tree has k particles in total. These configurations are all the combinations of (non-zero) integers that add up to k (this is, of course, what is required by mass conservation). This set of combinations is the *partitio numerum* of the integer k and, in general, there are a vast number of such combinations. If $Q(n)$ denotes the number of partitions of n, then the generating function of $Q(n)$ is

$$\sum_{n=0}^{\infty} Q(n)t^n = (1+t+t^2+\ldots)\ldots(1+t^k+t^{2k}+\ldots)\ldots = \prod_{k=1}^{\infty} \frac{1}{(1-t^k)}, \tag{49}$$

and, in the limit of large n,

$$Q(n) \sim \frac{1}{4n\sqrt{3}}\, \mathrm{e}^{\pi\sqrt{2n/3}} \tag{50}$$

(e.g. Abramowitz & Stegun 1964, section 24.2.1). It is easy to verify that equation (49) lists all possible partitions; the first set of brackets includes the contribution due to all possible sets of single particles, the second set of brackets includes the contribution due to all possible sets of pairs of particles, and the t^{nk} term includes the contribution due to n sets of the integer k. (For example, the decomposition 9=1+1+1+2+4 is given by the term $t^3t^2t^4$.)

Having listed all possible partitions, the second step is to assign probabilities to each partition. This is done by noting that the probability statements $f(j, \Delta_1|k, \Delta_2)$ for all $1 \leqslant j \leqslant k$ essentially provide a set of progenitors of size j given that the final clump is of size k. In other words, the statement $f(j, \Delta_1|k, \Delta_2)$ can be manipulated to give the probability that a progenitor is of size j, given that the final object is of size k. Since the different trees are just the different combinations of progenitors that give the final object of size k, the probability statements $f(j, \Delta_1|k, \Delta_2)$ contain some information about the probability that a particular tree structure occurs, given that the tree has k particles. The correct way to do this is shown below.

Let $p(l_1l_2\ldots l_m|k)$ denote the probability that the final clump with k particles at Δ_2 had the m progenitors, $\{l_1, l_2, \ldots, l_m\}$, at Δ_1. (Of course, $l_1 + l_2 + \ldots + l_m = k$. Also, note that $p(l_1l_2\ldots l_m|k)$ is independent of the order of $\{l_1, l_2, \ldots, l_m\}$ since different permutations of the 'branches' should all have the same probability of occurring.) It is relatively straightforward to show how to calculate this probability, though the calculation involves some complicated combinatorics.

First, note that the various $p(l_1l_2\ldots l_m|k)$ are not independent. This is because $p(l_1l_2\ldots l_m|k)$ denotes a probability, so the sum of $p(l_1l_2\ldots l_m|k)$ over all members of the *partitio numerum* of k should be properly normalized. Furthermore, since each $p(l_1l_2\ldots l_m|k)$ denotes a probability, all $p(l_1l_2\ldots l_m|k)$ must be positive definite for all choices of Δ_1 and Δ_2. Finally, notice that $f(j, \Delta_1|k, \Delta_2)$ involves summing over all trees that have at least one branch of size j.

The case when $k=1$ is trivial: the only possibility is that the single object at the final epoch was a single object previously, so that $p(1|1) = f(1|1) = 1$, where it is understood that $f(j|k)$ denotes $f(j, \Delta_1|k, \Delta_2)$. When $k=2$ there are two possible trees – they correspond to the two sets $\{2\}$ and $\{1, 1\}$. To calculate the probability that each occurs, use the fact that $p(2|2) = 2f(2|2)/2$ (where the factors of 2 in the numerator and the denominator on the right account for the fact that $f(2|2)$ counts the number of trajectories, and so the number of particles that are members of a clump of size 2, rather than the actual number of clumps of size 2), and the fact that it takes two single particles to make a pair, so that $2p(11|2) = 2f(1|2)/1$. Then $p(11|2) + p(2|2) = [f(1|2) + f(2|2)] = 1$, which follows from equation (41) for the normalization of the trajectories $f(j|k)$ with $k=2$. Similarly, $p(3|3)$, $p(21|3)$, and $p(111|3)$ are all uniquely determined by the $f(j|3)$, $j = 1, 2, 3$.

With just these few probabilities in hand it is possible to make a powerful statement about the structure of the merger history tree. One way to assign probabilities to each of the possible partitions is to use the generating function of partitions (equation 49) to write

$$\sum_{n=0}^{\infty} Q(n)t^n = \frac{(1+q_1(1)t+q_1(2)t^2+\ldots)}{1+q_i(1)+q_1(2)+\ldots} \cdots \frac{(1+q_k(1)t^k+q_k(2)t^{2k}+\ldots)}{1+q_k(1)+q_k(2)+\ldots} \cdots, \tag{51}$$

where $q_k(n)$ denotes the probability of having n sets of the integer k. Then the probability of the decomposition 9=1+1+1+2+4 is given by $q_1(3)q_2(1)q_4(1)/\prod_k(1+\sum_n q_k(n))$. For this procedure to work, $q_{l_m}(1)$ must equal $p(l_m|l_m)$ and $p(l_1, l_2, \ldots, l_m|l_1+l_2+\ldots+l_m) =$

Downloaded from https://academic.oup.com/mnras/article/276/3/796/1034602 by U.S. Department of Justice user on 17 August 2022

© Royal Astronomical Society • Provided by the NASA Astrophysics Data System

1995MNRAS.276..796S

$q_{l_1}(1)q_{l_2}(1)\ldots q_{l_m}(1)$ must hold if $l_1 \neq l_2 \neq \ldots \neq l_m$. However, $p(21|3) \neq p(2|2)p(1|1) = q_2(1)q_1(1)$, so that, from these first few terms, it is clear that a prescription like that required by equation (51) does not work.

It is not possible to continue the development initiated in the paragraph preceding equation (51) for arbitrarily large values of k. Although some of the probabilities can be determined uniquely (e.g., $p(k|k) = kf(k|k)/k$ for all k), it does not appear to be possible to solve for $p(l_1, l_2, \ldots, l_m|l_1 + l_2 + \ldots + l_m)$, for arbitrary $l_1, l_2, \ldots, l_m$, uniquely. This is because for a clump of size k there are $Q(k)$ unknowns representing the $Q(k)$ possible trees, but only k constraints, the $f(j|k)$: when $k \geqslant 4$, then $Q(k) > k$ (equation 49).

For example, when $k = 6$ then

$$
\begin{aligned}
\frac{6}{6} f(6|6) &= p(6|6),\\
\frac{6}{5} f(5|6) &= p(51|6),\\
\frac{6}{4} f(4|6) &= p(42|6) + p(411|6),\\
\frac{6}{3} f(3|6) &= 2p(33|6) + p(321|6) + p(3111|6),\\
\frac{6}{2} f(2|6) &= p(42|6) + p(321|6) + 3p(222|6) + 2p(2211|6) + p(21111|6),\\
\frac{6}{1} f(1|6) &= p(51|6) + 2p(411|6) + p(321|6) + 3p(3111|6) + 2p(2211|6) + 4p(21111|6) + 6p(111111|6),
\end{aligned}
$$

where, as before, the first factor of k/j on the left accounts for the fact that $f(j|k)$ counts the number of trajectories, and so the number of particles that are members of a clump of size j, rather than the actual number of clumps of size j (cf. the discussion of the previous subsection). Clearly, the requirement that $kf(j, \Delta_1|k, \Delta_2)/j$ involves a sum over all the $p(l_1 l_2 \ldots l_m|k)$ that include at least one j constitutes a powerful constraint on the choices of $p(l_1 l_2 \ldots l_m|k)$. When combined with the requirement that each $p(l_1 l_2 \ldots l_m|k)$ be positive definite for all choices of Δ_1 and Δ_2 (since they are probabilities), the $p(l_1 l_2 \ldots l_m|k)$ are even more severely constrained. However, there are insufficient constraints to specify the various tree probabilities uniquely.

The number of constraints increases if we make the following *ansatz*. Recall that the statements $f(j, \Delta_a|k, \Delta_b)$ are independent of what happened at times previous to Δ_a and also of what will happen at times later than Δ_b. Since the $p(l_1 l_2 \ldots l_m, \Delta_a|k, \Delta_b)$ are obtained from $f(j, \Delta_a|k, \Delta_b)$, assume that the dependence of $p(l_1 l_2 \ldots l_m, \Delta_a|k, \Delta_b)$ on Δ_a and Δ_b is the same for all choices of $\Delta_a \geqslant \Delta_b$. This *ansatz* is also suggested by the identities derived in equation (48). It provides a number of constraints that, for each k, take the form of functional equations that each $p(l_1 l_2 \ldots l_m, \Delta_a|k, \Delta_b)$ must satisfy. For example, since $p(22, \Delta_1|4, \Delta_3) = p(22, \Delta_2|4, \Delta_3)p(22, \Delta_1|22, \Delta_2) + p(4, \Delta_2|4, \Delta_3)p(22, \Delta_1|4, \Delta_2)$, where $\Delta_1 \geqslant \Delta_2 \geqslant \Delta_3$, requiring $p(22, \Delta_1|4, \Delta_3)$ to have the same dependence on Δ_1 and Δ_3 that $p(22, \Delta_2|4, \Delta_3)$ has on Δ_2 and Δ_3, and that $p(22, \Delta_1|4, \Delta_2)$ has on Δ_1 and Δ_2, provides a strong constraint on the functional form of $p(22|4)$. Imposing these constraints for arbitrary $p(l_1 l_2 \ldots l_m|k)$ involves straightforward, tedious algebra, so the details of the calculations are not presented here.

However, the $p(l_1 l_2 \ldots l_m|k)$ that satisfy these constraints on their functional forms can be manipulated to derive an analytic expression for the probability, $n(m|k)$, that a clump of size k (at the epoch corresponding to Δ_2) had exactly m progenitors (at the epoch corresponding to Δ_1). This follows from the fact that $n(m|k)$ is the sum over all the $p(l_1 l_2 \ldots l_m|k)$ that have the given value of m progenitors. [Just as each $f(j|k)$ is a sum over particular terms in the partition function, so too is each $n(m|k)$, though the terms in the sum that give $n(m|k)$ are different from those that give $f(j|k)$.]

When the constraints described above are imposed, then the probability that a clump of size k has m progenitors, one of which is of size j, is given by the term in $f(j|k)$ that is of order $(\Delta_1 - \Delta_2)^{m-1}$. So, expanding the polynomial in equation (40) and matching powers of $(\Delta_1 - \Delta_2)$ shows that

$$
\begin{aligned}
n(m|k) &= \frac{1}{m} \sum_{j=1}^{k-(m-1)} \binom{k}{j} \frac{j^{j-1}}{k^{k-1}} \left(\frac{1+\Delta_2}{1+\Delta_1}\right)^{k-1} \binom{k-j-1}{m-2} \left(\frac{k(\Delta_1 - \Delta_2)}{1+\Delta_2}\right)^{m-1} (k-j)^{k-j-m+1}\\
&= \frac{1}{m} \frac{k!}{(m-2)!} \left(\frac{\Delta_1 - \Delta_2}{1+\Delta_2}\right)^{m-1} \left(\frac{1+\Delta_2}{1+\Delta_1}\right)^{k-1} \frac{k^{m-k}}{(k-m)!} \sum_{i=0}^{k-m} \binom{k-m}{i} (i+1)^{i-1} (m-1+k-m-i)^{k-m-i-1}\\
&= \binom{k-1}{m-1} \left(\frac{\Delta_1 - \Delta_2}{1+\Delta_2}\right)^{m-1} \left(\frac{1+\Delta_2}{1+\Delta_1}\right)^{k-1}. \qquad (52)
\end{aligned}
$$

The $1/m$ factor accounts for the fact that each $p(l_1 l_2 \ldots l_{m-1} j|k)$ in the sum is counted m times. The final expression follows from the generalization of Abel's identity which is shown in equation (46).

This expression for $n(m|k)$, which derives from the requirement that the dependence of $p(l_1 l_2 \ldots l_m, \Delta_a|k, \Delta_b)$ on Δ_a and Δ_b is the same for all choices of $\Delta_a \geqslant \Delta_b$, has an interesting interpretation. Physically, it corresponds to requiring that in the limit of small time steps, that is, when $\Delta_a - \Delta_b$ is small, the probability that a clump has two progenitors should be an infinitesimal of first order, the probability of having three progenitors should be an infinitesimal of second order, and so on. This is a physically reasonable

Downloaded from https://academic.oup.com/mnras/article/276/3/796/1034602 by U.S. Department of Justice user on 17 August 2022

© Royal Astronomical Society • Provided by the NASA Astrophysics Data System

1995MNRAS.276..796S

requirement. Thus, the first factor in equation (52) is the number of ways of sorting k identical objects into m distinguishable clumps, subject to the constraint that none of the clumps remains empty. The second factor is the weighting for m progenitors, $(\Delta_1 - \Delta_2/A)^{m-1}$, where A is some constant. The final term is independent of m and corresponds to a normalization term. It follows from noting that $n(m|k)$ is a probability, and so must be normalized to unity, and from noting that $n(1|k) = p(k|k) = kf(k|k)/k$, which shows that $A = (1+\Delta_2)$. Finally, as $\Delta_1 \to \infty$, equation (52) shows that $n(m|k) \to 1$ for $m = k$ and $n(m|k) \to 0$ otherwise. This, too, is physically reasonable, since the progenitors at the epoch $\Delta_1 \to \infty$ of a k-sized clump at any epoch Δ_2 are all single particles.

Equation (52) shows how $n(m|k)$ is obtained from $f(j|k)$. Therefore, it must result from a set of progenitor tree probabilities, $p(l_1 l_2 \ldots l_m|k)$, that are consistent with the Poisson Press–Schechter trajectories, $f(j|k)$. Another way to verify the consistency of equation (52) is to calculate the total number density of progenitors (at epoch Δ_1) that it implies, since the average number density of clumps at Δ_1 is $\bar{n}(1-b_1)$ (cf. equation 2 and the relation obtained in Section 2.2). To do this, note that equation (52) implies that the average number of progenitors for a k-sized clump is

$$\sum_{m=1}^{k} m\, n(m|k) = \left(\frac{1+\Delta_2}{1+\Delta_1}\right)^{k-1} \sum_{m=1}^{k} m \binom{k-1}{m-1} \left(\frac{\Delta_1-\Delta_2}{1+\Delta_2}\right)^{m-1} = 1+(k-1)\left(\frac{\Delta_1-\Delta_2}{1+\Delta_1}\right) = \frac{b_1+k(b_2-b_1)}{b_2}, \tag{53}$$

where the sum is evaluated by making repeated use of the Binomial expansion. The final expression is obtained by expressing Δs in terms of bs (equation 19). The average number density of progenitor clumps that end up in clumps of size k is the number density of k-sized clumps, $\bar{n}(1-b_2)\,\eta(k,b_2)$, times the final expression in equation (53). Therefore, the average number density of progenitors is

$$\sum_{k=1}^{\infty} \bar{n}(1-b_2)\,\eta(k,b_2)\left(\frac{1+\Delta_2}{1+\Delta_1} + \frac{k(\Delta_1-\Delta_2)}{1+\Delta_1}\right) = \frac{\bar{n}\Delta_1}{1+\Delta_1} = \bar{n}(1-b_1), \tag{54}$$

as required.

Equation (53) for the average number of progenitors of a k-sized clump has an interesting consequence. It shows that, on average, the size of a progenitor of a k-sized clump is $kb_2/[b_1+k(b_2-b_1)]$. As required, for a given value of b_2, this average size decreases as b_1 decreases. It also has appropriate values in two limiting cases: the average size is unity when $b_1 = 0$, and is k when $b_1 = b_2$. Moreover, for those values of k for which

$$\frac{kb_2}{b_1+k(b_2-b_1)} > \frac{1}{(1-b_1)}, \tag{55}$$

the average progenitor size at the epoch b_1 is larger than the mean clump size at that epoch. This inequality is satisfied provided $k > 1/(1-b_2)$. However, $1/(1-b_2)$ is the mean clump size at the epoch b_2. Thus, equation (55) shows explicitly that the progenitors (at the epoch b_1) of clumps that are more massive than the mean at the epoch b_2 are themselves more massive, on average, than the mean clump size at the earlier epoch b_1.

It is possible to generalize equation (55) slightly. Require

$$\frac{kb_2}{b_1+k(b_2-b_1)} > \frac{1}{(1-\alpha b_1)}, \tag{56}$$

where α is some constant such that $0 \leqslant \alpha < 1/b_2$. This inequality is satisfied when $k > 1/(1-\alpha b_2)$. In other words, the average-sized progenitor identified at the epoch b_1 of a clump that, at the epoch b_2, is $(1-b_2)/(1-\alpha b_2)$ times more massive than the average clump size at that epoch is itself $(1-b_1)/(1-\alpha b_1)$ times more massive than the average-sized clump at the epoch b_1. This result shows explicitly that the partition function for merger history trees that is specified by requiring that the statements $p(l_1 \ldots l_m, \Delta_1|k, \Delta_2)$ have the same functional dependence on the epochs Δ_1 and Δ_2 for all choices of Δ_1 and Δ_2 requires that massive clumps form preferentially from massive progenitor clumps. Equation (56) quantifies the magnitude of this effect.

4.4 Relation to the scaling solution of Section 3.2

This subsection shows that the description of merging and hierarchical clustering from which equation (52) derives differs slightly from the description provided by the compound Poisson cluster PPSD model studied in Section 3.2.

Summing $n(m|k)\bar{\eta}(k,b_2)$ (obtained from equation 52) over all $k \geqslant m$ gives an expression for the probability that a clump has exactly m progenitors. If this probability is denoted $h(m;b_1,b_2)$, then the number density of clumps having exactly m progenitors is $\bar{n}(1-b_2)h(m;b_1,b_2)$, where

$$\begin{aligned} h(m;b_1,b_2) &= \sum_{k\geqslant m}^{\infty} \binom{k-1}{m-1}\left(\frac{b_1}{b_2}\right)^{k-1}\left(\frac{b_2-b_1}{b_1}\right)^{m-1}\frac{(kb_2)^{k-1}}{k!}\mathrm{e}^{-kb_2} \\ &= \frac{(b_2-b_1)^{m-1}}{m!}\sum_{k\geqslant m}^{\infty}\left(\frac{m\,k^{k-m-1}b_1^{k-m}\mathrm{e}^{-kb_1}}{(k-m)!}\right) k^{m-1}\mathrm{e}^{k(b_1-b_2)}. \end{aligned} \tag{57}$$

© Royal Astronomical Society • Provided by the NASA Astrophysics Data System

Downloaded from https://academic.oup.com/mnras/article/276/3/796/1034602 by U.S. Department of Justice user on 17 August 2022

1995MNRAS.276..796S

The term in brackets in the sum in the final expression is the Borel–Tanner distribution (e.g. Moran 1984), so equation (57) shows that $h(m;b_1,b_2)$ is closely related to the $(m-1)$th moment of the Borel–Tanner distribution.

The generating function of the $h(m;b_1,b_2)$ distribution is

$$H(s;b_1,b_2) \equiv \sum_{m=1}^{\infty} h(m;b_1,b_2)\, s^m = \sum_{k=1}^{\infty}\sum_{m=1}^{k} s^m \binom{k-1}{m-1} \left(\frac{b_1}{b_2}\right)^{k-1} \left(\frac{b_2-b_1}{b_1}\right)^{m-1} \frac{(kb_2)^{k-1}}{k!} \mathrm{e}^{-kb_2}$$
$$= \sum_{k=1}^{\infty} s k^{k-1} \frac{(b_1+b_2 s-b_1 s)^{k-1}}{k!} \mathrm{e}^{-kb_2}, \qquad (58)$$

where rearranging the order of the sums and then using the Binomial theorem has simplified the expression considerably. When $s=1$, $H(s;b_1,b_2)=1$ since $H(1;b_1,b_2)$ reduces to the sum that normalizes the Borel distribution. As a consistency check, calculate the first derivative of equation (58) with respect to s, and evaluate it at $s=1$. This is the first moment of $h(m;b_1,b_2)$: it is $\langle m\rangle \equiv (1-b_1)/(1-b_2)$. Since $b_2 \geqslant b_1$, this first moment is always greater than or equal to unity: $\langle m\rangle \geqslant 1$. As expected, it is identical to the expression that is obtained by averaging equation (53) over k, using the fact that k has a Borel distribution [that is, $\eta(k,b_2)$ is given by equation 2], and using the relation $b=1/(1+\Delta)$ (equation 19). Similarly, it is possible to calculate the jth derivative of equation (58) with respect to s, and evaluate it at $s=1$. This gives the jth factorial moment of the $h(m;b_1,b_2)$ distribution.

Now consider the compound Poisson PPSD model studied in Section 3.2. Equation (31) shows that, when the particles are in b_1-Borel clumps, then the clumps cluster (to form super-clusters) in such a way that the particle distribution is always described by the PPSD functional form. However, other than specifying the mean number of super-clusters, Section 3.2 did not provide a method for describing the probability that a super-cluster has some given number of b_1-Borel clumps. One way to estimate this distribution is to assume that, when the particle distribution is described by a Borel distribution with parameter $B=b_2$, then the generating function, $\eta(s,b_2)$, can be thought of as being obtained by compounding a clump size distribution, denoted $\gamma(m)$, with the size distribution, $\eta(N,b_1)$, of the b_1-Borel clusters. That is, $\gamma(m)$ is defined in such a way that

$$\eta(s,b_2) \equiv \sum_{N=1}^{\infty} \frac{(Nb_2)^{N-1}\mathrm{e}^{-Nb_2}s^N}{N!} = \mathscr{H}\Big(\eta(s,b_1)\Big) \equiv \sum_{m=1}^{\infty} \gamma(m)\, \Big(\eta(s,b_1)\Big)^m. \qquad (59)$$

The factorial moments of the $\gamma(m)$ distribution may be obtained by taking derivatives with respect to s on both sides of equation (59), and evaluating at $s=1$. Since these factorial moments also involve factorial moments of $\eta(s,b_1)$ and $\eta(s,b_2)$, and the factorial moments of a Borel distribution are known, equation (59) shows that the factorial moments of the $\gamma(m)$ distribution can be obtained, order by order, in closed form. Comparing these factorial moments of the $\gamma(m)$ distribution with the factorial moments of the $h(m;b_1,b_2)$ distribution shows that, except for the first moment, they are different. This means that $\gamma(m)$ and $h(m;b_1,b_2)$ have the same mean values, but are otherwise different. This difference increases as the difference between b_1 and b_2 increases. Thus, the evolution of hierarchical clustering that is implied by equation (52) differs from this simple approximation to the evolution described by the scaling solution model of Section 3.2.

The reason for the difference between the $\gamma(m)$ and $h(m;b_1,b_2)$ distributions is as follows. The merging history of Borel clumps, described by Sections 4.3 and 4.4, must evolve consistently with the fact that the initial distribution was Poisson. There is no such consistency requirement on the initial distribution of the Borel clumps in the compound Poisson PPSD model of Section 3.2. Moreover, the compounding process (equation 59) is only an approximate model for the way in which the b_1-Borel clumps must merge to make the $\eta(N,b_2)$ distribution. Essentially, this is because the compounding process assumes that $p(1\ldots 1|k) \propto \gamma(k)\eta(1,b_1)^k$, which conflicts with the results of the preceding section (cf. discussion following equation 51). It is this difference that causes the compounding approximation (equation 59) to the Section 3.2 description of the clustering of clumps to provide a different description from the more detailed, self-consistent model of Section 4.3.

4.5 Detailed model of hierarchical clustering

The results of Section 4.3 represent the exact solution to the problem that was studied using the approximate model of clustering developed in Section 3.4. This subsection shows how and when the approximate model (in which, to lowest order, clustering of Press–Schechter clumps occurs independently of the mass of the clumps) and the more detailed analysis of Section 4.3 differ.

Fig. 4 shows the $h(m;b_1,b_2)$ distribution (equation 57) for a number of representative values of b_1 and b_2, using linear and logarithmic scales. Solid curves show equation (57), and dotted curves show Borel distributions (equation 2) with $b=(b_2-b_1)/(1-b_1)$, for comparison. These dotted curves represent the approximate model of hierarchical clustering developed in Section 3.4. The solid curves that describe the exact distribution (equation 57) can be well approximated by a Borel distribution for most choices of b_1 and b_2. Let b_{eff} denote the value of b for which the Borel distribution fits the solid curves well. Fig. 4 shows that $b_{\mathrm{eff}} \approx (b_2-b_1)/(1-b_1)$ unless $b_1 \gtrsim 0.5$. This is consistent with the model developed in Section 3.4.

Recall that, by hypothesis, the Press–Schechter clumps (identified at the epoch b_2) have a Poisson spatial distribution (at the epoch b_2). Therefore, if the *ansatz* from which equations (52)–(58) derives is correct, then the counts-in-cells distribution function at the epoch b_2 of the Borel progenitor clumps identified at the epoch b_1 is given by compounding the $h(m;b_1,b_2)$ distribution with

Downloaded from https://academic.oup.com/mnras/article/276/3/796/1034602 by U.S. Department of Justice user on 17 August 2022

© Royal Astronomical Society • Provided by the NASA Astrophysics Data System

1995MNRAS.276..796S

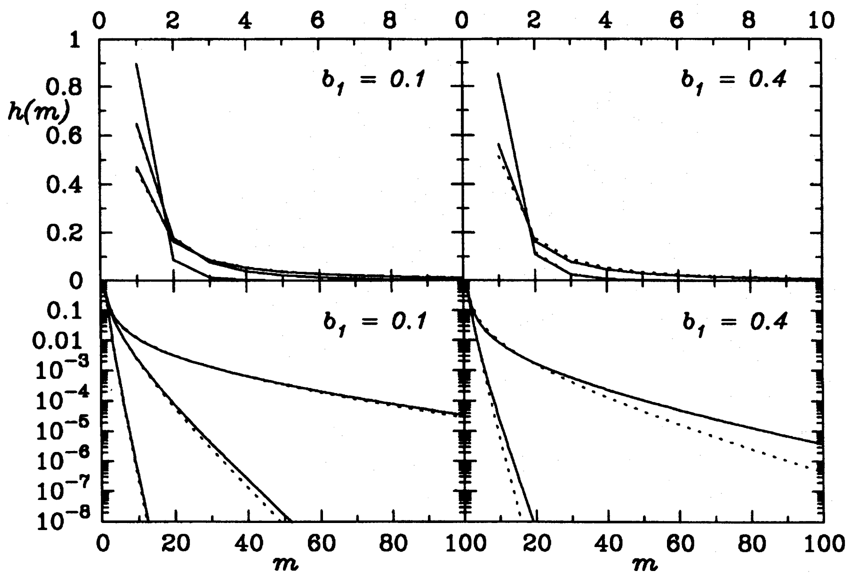

Figure 4. Equation (57) for a few representative values of b_1 and b_2, using linear and logarithmic scales. The panels with $b_1 = 0.1$ show curves for $b_2 = 0.2, 0.5$, and 0.8, and the panels with $b_1 = 0.4$ show $b_2 = 0.5$ and 0.8, respectively. In all the panels, as the difference $b_2 - b_1$ increases, the large-m tail increases. Solid curves show equation (57) and dotted curves show Borel distributions (equation 2) with $b = (b_2 - b_1)/(1 - b_1)$, for comparison. The dotted curves represent the approximate model of Section 3.4.

a Poisson distribution. Thus, at the epoch b_2, the distribution function of the number of Borel clusters (that were identified at the epoch b_1) in a randomly placed cell of size V is given by the recursion relation

$$P(N, \bar{n}_{\rm cl} V) = \sum_{m=0}^{N} \frac{P(N-m, \bar{n}_{\rm cl} V)}{N} \frac{\bar{n}_{\rm cl} V}{\langle m \rangle} m h(m; b_1, b_2) = \bar{N}(1 - b_2) \sum_{m=0}^{N} \frac{m}{N} P(N-m; \bar{n}_{\rm cl} V)\, h(m; b_1, b_2) \tag{60}$$

where $\bar{n}$ is the number density of particles, $\bar{N} \equiv \bar{n}V$, and $\bar{n}_{\rm cl} = \bar{n}(1 - b_1)$ is the number density of the Borel clusters identified at the epoch b_1. The first equality is a general result that holds for all compound Poisson distributions (e.g. Szapudi & Szalay 1993).

It is easy to verify that this counts-in-cells distribution has some appropriate properties. For example, the void distribution is given by $\exp[-\bar{N}(1 - b_1)/\langle m \rangle]$, where $\bar{N}(1 - b_1)$ is the average number of Borel progenitor clumps (that were identified at the epoch b_1) in a cell, and $\langle m \rangle$ is the mean number of those progenitor clumps that are in a Press–Schechter clump at the later epoch b_2. So, the void probability implied by equation (58) is $P(0) = \exp[-\bar{N}(1 - b_2)]$. As required, this is the same as $P(0)$ given by equation (1) at the epoch b_2. Further, recall that, by hypothesis, the spatial distribution of the Borel clumps that were identified at b_1 is Poisson when $b_2 = b_1$. Setting $b_1 = b_2$ in equation (58) shows that $H(s; b_1, b_2) \to s$ when $b_1 = b_2$. This is consistent with the requirement that the Borel clumps identified at b_1 have a Poisson spatial distribution initially (i.e., when $b_2 = b_1$). Finally, note that this compound Poisson distribution differs from a PPSD (equation 1) with parameter $(b_2 - b_1)/(1 - b_1)$. In other words, the functional form that describes the counts-in-cells distribution function of progenitor clumps differs from that which describes the particles.

However, Fig. 4 shows that, until m becomes very large, $h(m; b_1, b_2)$ is similar to $\eta(m, b_{\rm eff})$, where $b_{\rm eff} = (b_2 - b_1)/(1 - b_1)$, to within a few per cent for most values of b_1 and b_2. This means that, at least when the number of particles is small (i.e., $N_{\rm part}(1 - b_2) \lesssim 10^4$ or so), the Borel distribution, $\eta(m; b_{\rm eff})$, will provide a good approximate description, at the epoch corresponding to b_2, of the size distribution of clusters formed from the progenitor clumps that were identified at b_1. Now, recall that the PPSD is obtained by compounding a Borel distribution with a Poisson distribution. Therefore, when the Borel distribution, $\eta(m, b_{\rm eff})$, is a good approximation to the $h(m; b_1, b_2)$ distribution, then the PPSD, with parameter $b = b_{\rm eff}$, will provide a good approximate description of the spatial distribution (at the epoch b_2) of the Borel progenitor clumps (identified at b_1). That a PPSD with $b = b_{\rm eff} = (b_2 - b_1)/(1 - b_1)$ should fit the distribution of Borel clumps is consistent with the approximate model of the clustering of Press–Schechter clumps that was developed in Section 3.4.

Fig. 5 shows the counts-in-cells distribution function for Borel clumps identified at the epoch b_1, for a range of choices of scale (parametrized by the average number of particles in a cell, $\bar{N}$), and of the epochs b_1 and b_2. The solid lines show the theoretical distribution function computed numerically using equations (57) and (60). As described above, this distribution function derives from an exact treatment of the merging history of the Press–Schechter clumps. It describes the clustering of the Borel clusters under the assumption that, in the limit of small time steps, the probability that a clump is involved in a binary merger is an infinitesimal, the probability that a clump merges with two other progenitor Borel clumps is an infinitesimal of the next higher order, and so on. The dashed lines show a Poisson distribution with the same $\bar{N}$ for comparison. Since the number density of

Downloaded from https://academic.oup.com/mnras/article/276/3/796/1034602 by U.S. Department of Justice user on 17 August 2022

© Royal Astronomical Society • Provided by the NASA Astrophysics Data System

1995MNRAS.276..796S

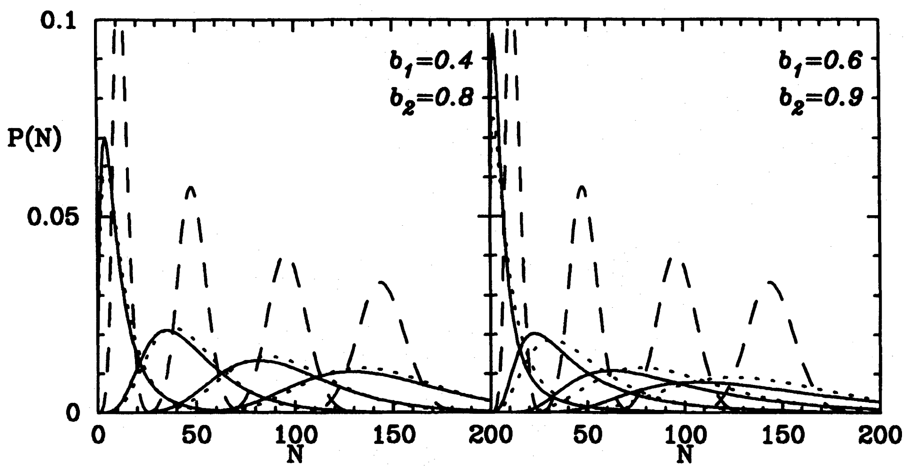

Figure 5. Comparison of models of the clustering, at the epoch b_2, of Borel clumps that were identified at the earlier epoch b_1. Solid lines show the exact Press–Schechter merging history description (equations 57 and 60), and dashed lines show a Poisson distribution for comparison. Dotted lines show that, for all choices of b_1 and b_2, a PPSD with $b_{\rm eff} = (b_2 - b_1)/(1 - b_1)$ provides an excellent fit to the exact result. These dotted lines represent the approximate model of hierarchical clustering that was developed in Section 3.4. From left to right, the curves have $\bar{N} = 20, 80, 160$, and 240, for the $b_1 = 0.4$ panel, and $\bar{N} = 30, 120, 240$, and 360, for the $b_1 = 0.6$ panel.

Borel clumps identified at the epoch b_1 is $\bar{n}(1 - b_1)$, the peak of the Poisson distributions occurs at $\bar{N}(1 - b_1)$. When the difference between b_1 and b_2 is small, then the solid curves are close to the Poisson curves. This is expected since, by hypothesis, the Borel clumps have a Poisson distribution at the epoch b_1. The solid curves become increasingly different from the Poisson (dashed) curves as the difference between b_2 and b_1 increases.

The dotted lines in Fig. 5 show PPSDs that have $b = (b_2 - b_1)/(1 - b_1)$. If the approximate description of Section 3.4 is accurate, they should provide good fits to the solid curves on all scales. The figure shows that for all choices of b_2 and $\bar{N}$ these dotted PPSD curves, with $b_{\rm eff} = (b_2 - b_1)/(1 - b_1)$, provide good fits to the solid lines, at least when $b_1 \lesssim 0.4$. As b_1 increases, the dotted curves become less skewed (and more Poisson-like) than the solid curves. This shows that the approximate model of Section 3.4, which assumed that, to lowest order, the clustering of Borel clumps occurs independently of the mass of the clumps, differs slightly from the more exact merger history model developed in this section. The extent to which this assumption breaks down is quantified by the difference between the solid and the dotted curves.

Although the fits with $b_{\rm eff} = (b_2 - b_1)/(1 - b_1)$ become worse for larger b_1, the PPSD continues to provide a relatively good description provided $b_{\rm eff}$ is allowed to exceed $(b_2 - b_1)/(1 - b_1)$. This means that, for all choices of b_1, b_2, and $\bar{N}$, the PPSD functional form provides an excellent approximation to the exact distribution defined by equations (57) and (60). Thus, Fig. 5 shows that, on all scales, the spatial distribution, at the epoch b_2, of the Borel clumps that are identified at the epoch b_1 is well approximated by a PPSD with some effective value of $b_{\rm eff} \gtrsim (b_2 - b_1)/(1 - b_1)$, for all choices of b_1 and b_2. This suggests the following simple model of hierarchical clustering from an initially Poisson distribution.

At any epoch, say b_1, the distribution of particles is described by a PPSD distribution, with parameter b_1. This distribution can be understood as a Poisson distribution of Press–Schechter clumps, in which the distribution of clump 'masses' is given by a Borel distribution with parameter b_1 (cf. Sections 2.1 and 2.2). To a good approximation, rather than considering the details of the internal structure within each Borel clump, the clumps described by the Borel cluster decomposition may be replaced by point-shaped objects of the appropriate mass located at the centre-of-mass of the clump (cf. Section 3.2). At some later epoch, say b_2, the particle distribution is described by a PPSD distribution with parameter b_2, and so it can be understood as a Poisson distribution of Borel clumps with parameter b_2. This means that, by the epoch b_2, the b_1 clumps have all merged to form the b_2 clumps. The spatial distribution of the b_1 clumps, at the epoch b_2, is given by equations (57)–(60). However, this distribution is well approximated by a PPSD with parameter $b_{\rm eff} \approx (b_2 - b_1)/(1 - b_1)$. In this model, therefore, clustering from an initially Poisson distribution is both hierarchical and stable: at any epoch the distribution of particles is a PPSD, and the distribution of the Borel, Press–Schechter clumps that were identified at any previous epoch is also (approximately) a PPSD.

5 COMPARISON WITH *N*-BODY SIMULATIONS

In this section a number of the analytic results of the previous sections are tested using *N*-body simulations of non-linear gravitational clustering from Poisson initial conditions, kindly made available by Dr M. Itoh and Professor S. Inagaki. The distribution functions of particle counts in randomly placed cells that are measured in these simulations are extremely well fitted by the PPSD of equation (1) (Itoh, Inagaki & Saslaw 1988, where these simulations are described in greater detail). This measured

Downloaded from https://academic.oup.com/mnras/article/276/3/796/1034602 by U.S. Department of Justice user on 17 August 2022

© Royal Astronomical Society • Provided by the NASA Astrophysics Data System

1995MNRAS.276..796S

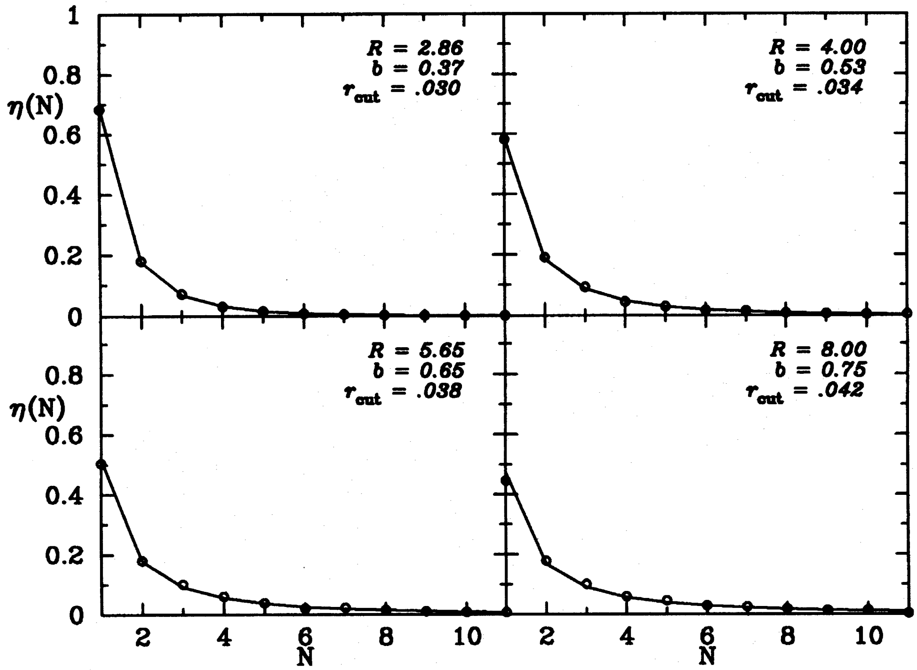

Figure 6. Fraction, $\eta(N)$, of friends-of-friends clusters having exactly N particles (open circles), compared with a Borel distribution with the appropriate value of b (solid lines), for a range of expansion factors, R.

agreement provides some support for the Press–Schechter theory developed in Section 2. A more direct comparison is to compute the mass spectrum for the simulations, and to compare it with the Borel distribution (equation 2) predicted by this Press–Schechter approach (Section 2.1). Section 5.1 is devoted to this comparison. All these results depend on the evolution of the overdensity threshold, Δ, calculated in Section 2.3. equations (22) and (24) for the evolution of b are in very good agreement with the measured evolution of the variance in relevant N-body simulations of gravitational clustering (fig. 1 in Zhan 1989). Therefore, to very good accuracy, the evolution of Δ is given by equation (25), so there are no free parameters in the comparison of the analytic results with the simulations. Section 5.2 compares the approximate model of hierarchical clustering developed in Section 3.4, and the more exact model developed in Sections 4.3 and 4.4, which is based on the merging histories of the Press–Schechter clumps, with the N-body results. In Section 5.3, counts-in-cells distribution functions from N-body simulations, in which particles are not identical but have a range of masses, are used to test the merger history model of Sections 4.3 and 4.5 further.

5.1 Clusters in the simulations

Using a friends-of-friends algorithm, this subsection constructs group catalogues for the N-body simulations in which identical particles initially have a Poisson spatial distribution. Then it compares the group catalogues (computed for a range of expansion factors) with the Borel decomposition of the PPSD. The agreement is excellent, demonstrating that the Borel decomposition describes physical clusters, and suggesting that the PPSD, and so the Press–Schechter approach, provides a very good description of the non-linear gravitational clustering in these simulations.

When the number density of particles is $\bar{n}$, then the number density of Borel clusters is $\bar{n}(1-b)$, and b in the Borel distribution of equation (2) is determined by the large-scale value of the variance. At any given epoch in the N-body simulations the link length, say r_{cut}, that determines the friends-of-friends cluster catalogue is chosen so that it gives the correct number density of cluster centres, $\bar{n}(1-b)$, for a given value of the variance. Recall from Section 2.3 that the variance on large scales can be calculated from linear theory, and that a given value of the large-scale variance determines a value of b, so that, in principle, this choice of r_{cut} is determined by linear theory. From this cluster catalogue it is straightforward to calculate the fraction of clusters that have exactly N particles.

The open circles in the four panels of Fig. 6 show the probability, $\eta(N)$, that a friends-of-friends cluster has N particles. Each panel also shows the expansion factor, R, the value of b determined directly from the variance of the counts-in-cells (cf. Section 2.3), and the corresponding value of r_{cut} (which is in units with the diameter of the simulation sphere scaled to unity) that gives the correct number density of friends-of-friends clusters. The solid lines through the circles show the Borel distribution with the same value of b; it provides an excellent fit at all expansion times shown. Thus, Fig. 6 suggests that the Borel decomposition of the PPSD is not merely a mathematical nicety; rather, it describes clusters that are real physical entities.

Replacing each friends-of-friends cluster by its centre of mass and computing the two-point correlation function for the

Downloaded from https://academic.oup.com/mnras/article/276/3/796/1034602 by U.S. Department of Justice user on 17 August 2022

© Royal Astronomical Society • Provided by the NASA Astrophysics Data System

1995MNRAS.276..796S

Table 1. Spatial distribution, at a later epoch (expansion factor R_2), when the particle distribution is a PPSD with parameter B, of Press–Schechter clumps identified at an earlier epoch (expansion factor R_1), when the particle distribution was a PPSD with parameter b. For all cell sizes, and for all values of b and B, the spatial distribution of these b-Borel, Press–Schechter clumps is well approximated by a PPSD with parameter $b_{\rm fit} \gtrsim (B-b)/(1-b)$. This last is termed $b_{\rm cen}$. The approximate model developed in Section 3.4 suggests that $b_{\rm fit} = b_{\rm cen}$, whereas Section 4.4 argues that $b_{\rm fit} \gtrsim b_{\rm cen}$ is more accurate.

R_1	R_2	b	B	$b_{\rm fit}$	$b_{\rm cen}$
2.9	2.9	0.37	0.37	0.02	0.00
2.9	4.0	0.37	0.53	0.28	0.25
2.9	5.6	0.37	0.65	0.50	0.44
2.9	8.0	0.37	0.75	0.65	0.60
2.9	16.0	0.37	0.87	0.81	0.79
4.0	4.0	0.53	0.53	0.01	0.00
4.0	5.6	0.53	0.65	0.32	0.26
4.0	8.0	0.53	0.75	0.53	0.47
4.0	16.0	0.53	0.87	0.77	0.72
5.6	5.6	0.65	0.65	0.03	0.00
5.6	8.0	0.65	0.75	0.36	0.29
5.6	16.0	0.65	0.87	0.70	0.63
8.0	8.0	0.75	0.75	0.02	0.00
8.0	16.0	0.75	0.87	0.55	0.48

resulting point distribution shows that the cluster centres are not correlated with each other. Furthermore, the counts-in-cells distribution function of this centre-of-mass distribution is Poisson, as required by the Poisson cluster decomposition discussed in the introduction, and assumed in the Press–Schechter derivation. The excellent agreement of the Borel cluster decomposition with the friends-of-friends clusters shown in Fig. 6 suggests that the PPSD functional form, and so the Press–Schechter approach, provides an excellent description of non-linear clustering from an initially cold Poisson distribution of identical particles.

5.2 Clustering of identical particles

The similarity of the excursion set distributions of an initially Poisson distribution and of the compound Poisson PPSD model suggests an interesting scaling when applied to the clustering of the Borel cluster centres that arise as the initially Poisson distribution begins to cluster. In particular, Section 3.4 suggests the following model.

It is possible to follow the evolution of the friends-of-friends/Borel cluster centres identified at, say, $R = 2.86$ of an initially Poisson distribution. If the clustering is stable and hierarchical, as the results of the previous subsection suggest, then, since b increases as clustering develops so that the number density of clusters, $\bar{n}(1-b)$, decreases, these clusters should, on average, combine to form the (Poisson distributed) friends-of-friends/Borel clusters that are identified at later epochs. The approximate model developed in Section 3.4 argues that if the friends-of-friends/Borel clusters are identified at, say, $R = 2.86$, so that $b_{\rm cen}$ for these clusters is zero at $R = 2.86$ (i.e., their spatial distribution at $R = 2.86$ is Poisson), then at some later time these cluster centres will themselves have clustered in such a way that, while the distribution function of the individual particles continues to be described by a PPSD with some (increasing) value of $B > b$, the distribution function of the Borel centres is also approximately a PPSD with some (increasing) non-zero value of $b_{\rm cen} = (B-b)/(1-b) < B$.

The approximate model of Section 3.4 was derived under the assumption that the clustering of the Borel clumps occurred without regard for the mass of the clumps. The more exact treatment of Sections 4.3 and 4.4 (Figs 4 and 5) showed that, in fact, this approximation is both useful and surprisingly accurate (at least for small values of b_1). Section 4.4 showed that, in general, counts-in-cells analyses at the epoch B of clumps identified at the epoch b should be well approximated by a PPSD with $b_{\rm fit} \gtrsim (B-b)/(1-b)$.

The simulations discussed in the previous subsection can be used to make a crude test of this prediction. There are at least two ways in which this can be done. One way is to construct a friends-of-friends catalogue that has $\bar{N}(1-b)$ clusters at the epochs b and B. Then verify that each b-Borel cluster at the epoch B has exactly the same member particles that it had when it was identified at the epoch b. Finally, replace each cluster by its centre of mass, and compute the counts in cells distribution function of the resulting point distribution. A quicker way is to assume that the cluster members identified at the epoch b remain bound to each other, in the same cluster, at the epoch B. (Of course, this is consistent with the models of Sections 3.4 and 4.4.) So, the

Downloaded from https://academic.oup.com/mnras/article/276/3/796/1034602 by U.S. Department of Justice user on 17 August 2022

© Royal Astronomical Society • Provided by the NASA Astrophysics Data System

1995MNRAS.276..796S

centre of mass, at the epoch B, of each cluster that was identified at the epoch b is given simply by calculating the appropriate average over the positions (at the epoch B) of all the member particles. (This method is quicker than the previous one because here there is no check that the members of a cluster identified at the epoch b remain members at the later epoch B.) Then compute the new distribution function for these b clusters and the later epoch B. If the models of Sections 3.4 and 4.4 are correct, then the distribution should be Poisson at the epoch b, whereas it should be well approximated by a PPSD, with $b_{\rm fit} \gtrsim (B-b)/(1-b)$, at the epoch B.

Table 1 shows the results of applying this quicker, cruder test to the N-body simulations for a range of values of b and B. For all values of b and B considered, the PPSD provides excellent fits to the cluster centre distributions. These fits are not reproduced here. The table shows the values of $b_{\rm fit}$ that provide good fits to the distribution functions – they are calculated directly from the variance of the counts (cf. Sheth & Saslaw 1994). Usually the value of $b_{\rm fit}$ is determined to within five per cent of its value. The column on the far right shows the corresponding value of $b_{\rm cen} \equiv (B-b)/(1-b)$, as suggested by the model of Section 3.4.

For example, Table 1 shows that, when the expansion factor is $R_2 = 8.00$, then the distribution function of the Press–Schechter clumps defined at $R_1 = 2.86$ is well described by a PPSD with a value of $b_{\rm fit}$ that is zero when the clusters are identified (i.e., at $R_1 = 2.86$ and $b \approx 0.37$) and $b_{\rm fit}$ does indeed increase as the simulation evolves further. In particular, $b_{\rm fit} \approx 0$ when $R_2 = 2.86$ and $b_{\rm fit} \approx b_{\rm cen}$ when $R_2 = 8.00$ and $B \approx 0.75$. This shows that, within the uncertainties, the model of Section 3.4 provides a good description of the clustering of the Borel clusters provided that $b \lesssim 0.4$. Thereafter, $b_{\rm fit} \gtrsim b_{\rm cen}$, with the difference increasing systematically as b increases. This is consistent with the more detailed model developed in Section 4.4.

Only at very late times (expansion factor $R \gtrsim 30$), when it is not clear that the simulations are statistically homogeneous anyway, and there are fewer clumps from which to compute the statistics accurately, do the distribution functions of the friends-of-friends clusters (i.e., the ones identified at, say, $R = 2.86$) depart substantially from a PPSD. This shows that, to a good approximation, the gravitational clustering in these simulations is both stable and hierarchical, and that the clustering occurs in a self-similar manner, since the same functional form that describes the clustering of the original particles also describes the distribution of the friends-of-friends clusters. This suggests that it is a reasonably good approximation to replace the friends-of-friends/Borel clusters by their centres-of-mass; i.e., the details of the smaller scale structure within the average cluster do not significantly affect the statistical properties of the clustering on larger scales.

We conclude this section with the following observation. That the distribution of the Borel clumps is well described by a PPSD with $b_{\rm cen} \approx (B-b)/(1-b)$ is consistent with the model of merging and hierarchical clustering developed in Section 4.3 (cf. Fig. 5). Therefore, the results of this subsection suggest that the procedure, developed in Sections 4.3 and 4.4, by which merger history trees should be constructed is, substantially, correct.

5.3 Effects of continuous mass spectra

The model of the evolution of gravitational clustering from Poisson initial conditions (i.e., the model developed in Sections 3.2, 4.3 and 4.4 and tested in the previous subsection) also provides a simple explanation for the results of Itoh et al. (1993). They studied gravitational clustering in a range of systems with Schechter-type initial mass spectra, i.e.,

$$\mathrm{d}N \propto \left(\frac{m}{m_*}\right)^{-p} \mathrm{e}^{-(m/m_*)}\, \mathrm{d}\left(\frac{m}{m_*}\right) \tag{61}$$

(Schechter 1976), for which the initial spatial distribution of the particles (with different masses) was Poisson. That is, they studied the evolution of gravitational clustering for a distribution that, initially, is a compound Poisson cluster distribution, so that the Press–Schechter type model developed in Section 3 may apply to these simulations.

In particular, the results of Section 3.2 suggest that, provided the parameters p and m_* of the Schechter mass function are chosen so that the resulting distribution of masses is similar to a Borel distribution (with some value of b), the clustering will always be well approximated by the PPSD form. That is, if a clump of mass Nm is counted as having N times the number of particles as a clump of size m, then the counts-in-cells distribution of the mass will be well approximated by the PPSD form. Section 3.2 argued that when the distribution of identical particles (i.e. all particles have the same mass) is a PPSD with some parameter B, and the particles are bound up in b-Borel clumps (with $b \leqslant B$), then the clustering of the cluster centres is also well approximated by a PPSD [with $b_{\rm cen} \approx (B-b)/(1-b)$]. This means that, at least at early times, the clustering of the multimass particles in the Schechter mass models will be qualitatively and quantitatively similar to the late-time evolution of the clustering of the Borel clumps in the single-mass simulations (i.e., at times after the value of b that is similar to the Schechter mass distribution has been reached).

Therefore, it is of interest to determine the range, if any, of parameters for which the Schechter function is similar to a Borel distribution. That some range does exist is shown by the limiting case of equation (11). The expression that results is similar in form to the function proposed by Press & Schechter (1974, their equation 13) for a distribution evolved from Poisson initial conditions, from which the Schechter distribution in equation (61) was derived.

In their work, Itoh et al. (1993) studied a variety of models with $p = 0$–5. All models had mass ranges between $m_{\rm min}/m_* = 0.01$ and $m_{\rm max}/m_* = 10.0$ with the additional requirement that all models have the same total mass. Fig. 7 shows the shape of the

Downloaded from https://academic.oup.com/mnras/article/276/3/796/1034602 by U.S. Department of Justice user on 17 August 2022

© Royal Astronomical Society • Provided by the NASA Astrophysics Data System

1995MNRAS.276..796S

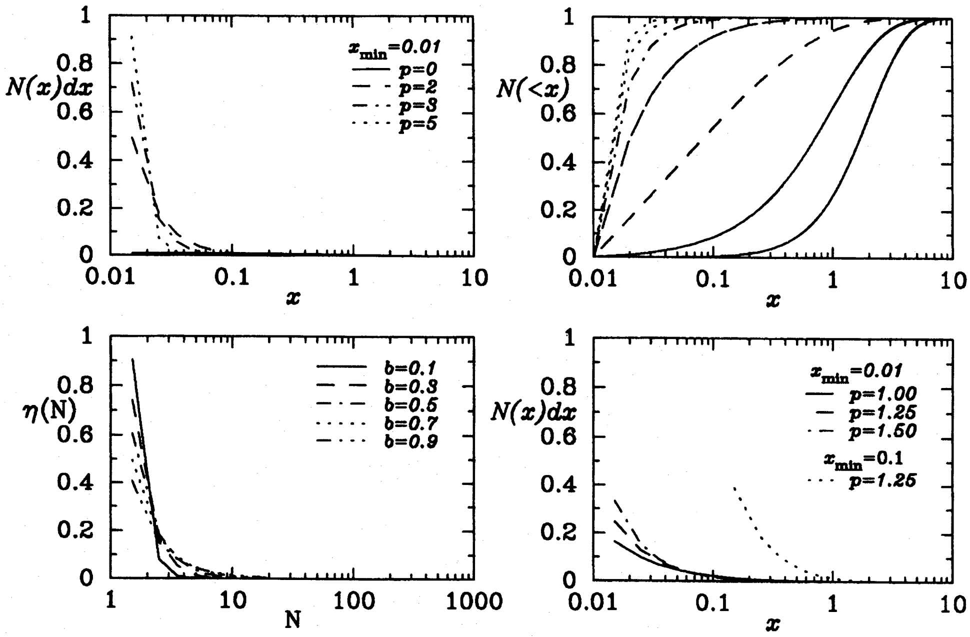

Figure 7. Top left shows the Schechter mass function, $N(x)\,\mathrm{d}x$ with $x \equiv m/m_*$, binned in units of the smallest mass ($x_{\rm min} = m_{\rm min}/m_*$), as a function of normalized mass x. Top right shows the corresponding cumulative mass (lower curves of each line style) and number (upper curves of each line style) distributions for the Schechter models. The line styles in this panel represent the same parameter choices as in the top left panel. Bottom left shows the Borel distribution, $\eta(N,b)$, for a range of b values; the mass range increases as b increases. Bottom right shows another set of Schechter mass functions, with parameters as shown. For many choices of the parameters p and $x_{\rm min}$ the shape of the Schechter functions is similar to that of the Borel distributions.

Schechter mass function, $N(x)\,\mathrm{d}x$ with $x \equiv m/m_*$, binned in units of the smallest mass ($x_{\rm min} = m_{\rm min}/m_*$) for the models studied by Itoh et al. It shows that, for a wide range of parameters, the Schechter mass function is similar to a Borel distribution, $\eta(N,b)$. Moreover, Fig. 7 shows that agreement of the Schechter-mass simulations with the PPSD functional form will not be monotonic with p. Whereas models with $1 \lesssim p \lesssim 2$ have a mass range that is slightly broader than most of the Borel distributions, models with large values of p are more similar to the Borel form.

The Itoh et al. (1993) results show that the clustering of the multimass particles in those models where the initial Schechter mass function is similar to a Borel distribution (with some effective value of b) is well described by a PPSD until relatively late stages of clustering, whereas models that are initially quite different from a Borel distribution show departures from the PPSD model at relatively early epochs. This qualitative feature is precisely what is expected for the Poisson cluster description of clustering developed in Section 3.2, and can be considered as a success of that Press–Schechter type approach in describing the gravitational evolution of these multimass model simulations.

Furthermore, the equivalence between clustering in those multimass models for which the Schechter mass function resembles a Borel distribution, and the late-time clustering in the single-mass simulations studied in the previous two subsections (suggested by the results in Section 3.2 and the measured accuracy of the PPSD functional form in describing the clustering of these multimass particles) can be used to test the hierarchical clustering model developed in Section 4.5 with greater dynamic range than was possible in Section 5.2. The good fit of the PPSD to these multimass models at earlier times, with the accuracy of the fit decreasing at late times, is consistent with the model developed in Section 4.5. Thus, the Itoh et al. (1993) results strongly suggest that the prescription, obtained in Section 4.3, for constructing merger history trees is, substantially, correct.

6 DISCUSSION AND CONCLUSIONS

Equation (1), which fits the observed galaxy counts-in-cells distribution function, was predicted by the thermodynamic model developed by Saslaw & Hamilton (1984). Section 2 of the present paper presented a new derivation of this functional form that was effected without any explicit consideration of an underlying thermodynamics. Using the earlier work of Press & Schechter (1974), and of Epstein (1983), Section 2 showed that the Borel distribution, and so equation (1), can be derived from a Press–Schechter type description of the non-linear clustering of an initially Poisson distribution of identical particles. Therefore, when studying the gravitational evolution of large-scale structure in the universe, the intimate relation between the Poisson distribution and equation (1) means that equation (1) is interesting whether or not the thermodynamic theory developed by Saslaw & Hamilton (1984) applies. Section 2.2 termed equation (1) the Poisson Press–Schechter distribution function (PPSD). Section 2.3 computed the

Downloaded from https://academic.oup.com/mnras/article/276/3/796/1034602 by U.S. Department of Justice user on 17 August 2022

© Royal Astronomical Society • Provided by the NASA Astrophysics Data System

1995MNRAS.276..796S

temporal evolution of gravitational clustering in this Poisson Press–Schechter model; the result does not require any assumptions about the details of the spherical collapse, and describes cosmological models with arbitrary values of the density parameter, Ω.

Section 3 extended this result to apply to generic compound Poisson distributions (discussed by Sheth & Saslaw 1994), such as the PPSD and the Negative Binomial distributions. In this respect, Section 3 extends the results of Lucchin & Matarrese (1988) who tried to compute the cluster multiplicity functions for the PPSD and the Negative Binomial distributions. They obtained expressions that were valid only in the very massive clump limit. Section 3 showed how to obtain the multiplicity functions for clumps of arbitrary mass, for this class of non-Gaussian distributions, exactly. The analysis presented there also showed clearly that the development of merging and hierarchical clustering from an initially compound Poisson distribution can be described analogously to the treatment presented in Section 4 for the simple Poisson distribution.

One result of Section 3 is of particular interest. For the special case when the compound Poisson model has the PPSD form, the resulting excursion set cluster multiplicity function description simplifies considerably. Section 3.2 showed that the Press–Schechter description of non-linear clustering from a distribution of particles that is, initially, a PPSD is identical in form to, and differs only by a scaling factor from, the description of clustering from an initially Poisson distribution. This expression (equation 31) for the excursion set mass functions of a PPSD also solves, exactly, the problem posed by Rephaeli & Saslaw (1986) of describing the gravitational evolution of correlated fluctuations. It quantifies their schematic analysis which suggested that the natural growth of correlated fluctuations leads to much faster growth of hierarchical clustering than is the case for Poisson fluctuations.

In particular, the scaling solution obtained in Section 3.2 suggests that, if the Press–Schechter approach describes the effects of gravity, then non-linear gravitational clustering from an initially Poisson distribution of identical particles develops, to a good approximation, through a stable, hierarchical series of PPSD distributions: clustering on every level of the hierarchy is well approximated by the PPSD form. It also suggests that the spatial distribution after non-linear clustering from a distribution that is initially a compound Poisson PPSD is similar to that from an initially Poisson distribution. However, the evolution of the clustering is accelerated relative to the Poisson case. Sections 5.1 and 5.2 showed that both these predictions of this Press–Schechter type description of non-linear clustering were in qualitative agreement with the evolution of friends-of-friends clusters measured in relevant N-body simulations of gravitational clustering. Although Section 5 compared the analytic results of Sections 2 and 3 with N-body simulations of an $\Omega = 1$ cosmology only, the measured good agreement of the PPSD form (equation 1) with counts-in-cells analyses in low-Ω cosmologies (Itoh et al. 1988; Zhan 1989) shows that Sections 2 and 3 describe clustering in these less dense cosmologies also.

These results also allow a quantitative description of the development of hierarchical clustering through merging for the case of a Poisson (rather than a Gaussian) distribution. In Section 4 the first step towards a description of the entire merging history tree was formulated and solved. The technique used was similar to that of Bond et al. (1991) and of Lacey & Cole (1993). The result gave the probability that a clump of exactly, say, j particles at a given early epoch is later in a larger, more massive clump of exactly, say, k particles. Unfortunately, the N-body simulations analysed in Section 5 have only 10^4 particles, so they do not have enough resolution to test the merger results. Therefore, the analytic results of Section 4.1, which describe the merger rates of Press–Schechter clumps, will be compared with larger simulations in a future work. However, the demonstrated close relation between these results and those of Lacey & Cole (1993), and the measured agreement of the Lacey & Cole expressions with relevant N-body simulations (Lacey & Cole 1994), suggests that the results of this work will describe the development of merging and hierarchical clustering from Poisson initial conditions very well.

Section 4.3 showed how to calculate the partition function of the merger history tree. It showed that this partition function cannot be obtained in a closed form without additional assumptions. These assumptions are analogous to those made by Kauffmann & White (1993) in their Monte Carlo treatment of this problem. Section 4.3 assumed that the functional dependence on the initial and final epochs of the probability that a particular tree structure occurs is the same for all choices of epochs. This assumption is consistent with all other results of the Press–Schechter approach. Section 4.3 showed that the consequences of this assumption are physically reasonable. In particular, it showed that one consequence of this assumption is that in the limit of very small time steps the probability that a clump has two progenitors is an infinitesimal, the probability that the clump has three progenitors is an infinitesimal of the next higher order, and so on. Section 4.3 also showed that, for any given halo size, this assumption specifies the distribution of the number of progenitor clumps as a function of redshift, completely (equation 52). Equation (52) was shown to have physically reasonable properties, and to imply that massive clumps form preferentially from massive progenitor clumps (equation 55). In particular, equation (55) represents an analytic statement of the fact, observed in Monte Carlo studies of merger histories by Kauffmann (1995), that, on average, the size, at some earlier epoch, of the largest progenitor clump of a clump at some given final epoch depends significantly on how massive the final clump is relative to the characteristic mass at the final epoch.

Although this distribution of the number of progenitor clumps (identified at some initial epoch) that merge to form a given halo (at some final epoch) has yet to be tested directly with N-body simulations, Section 4.5 showed how to use it to calculate the distribution function of counts of progenitor clumps in randomly placed cells that it implies. It showed that, at least at relatively early times, this distribution function was well approximated by a PPSD that has an effective value of b that depends on the initial and final epochs (Fig. 5).

Section 5.3 showed how to use the simulations of Itoh et al. (1993), in which particles that initially have a Poisson spatial distribution are not identical but have a range of masses, to provide an indirect test of the predictions of Sections 4.3–4.5. It

Downloaded from https://academic.oup.com/mnras/article/276/3/796/1034602 by U.S. Department of Justice user on 17 August 2022

© Royal Astronomical Society • Provided by the NASA Astrophysics Data System

1995MNRAS.276..796S

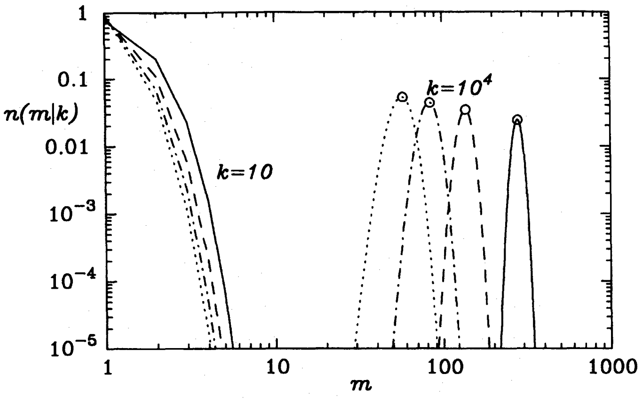

Figure 8. Distribution of the number, m, of progenitor clumps at a given initial epoch, for two choices of the final clump size, k. As explained in the text, this distribution, $n(m|k)$, is shown for a variety of choices of initial and final epochs, Δ_1 and Δ_2. For $k = 10^4$, curves corresponding to lower values of Δ_2 are broader (dotted, dot-dashed), and peak at lower values of m than those with larger values of Δ_2 (dashed, solid). Open circles at the peaks of the curves show $n(\bar{m}|k)$ where $\bar{m}$ is the mean number of progenitor clumps for the chosen values of k, Δ_1, and Δ_2. This mean value is given by equation (53).

argued that the compound Poisson cluster model studied in Section 3.2 could be used to describe the growth of clustering in the multimass simulations, provided that the distribution of mass sizes is similar to a Borel distribution. Fig. 7 showed that the mass distributions in some of the Itoh et al. models are, indeed, well approximated by Borel distributions. For these models, it argued, the clustering of the multimass particles should be well approximated by the PPSD functional form, for the same reason that the clustering of Borel clusters in the single-mass simulations is well approximated by a PPSD (Section 5.2, Table 1). Thus, it argued, the multimass simulations can be understood as extending the dynamic range of the single-mass simulations. Finally, it argued that the good fit of the PPSD to these multimass models at earlier times, with the accuracy of the fit decreasing at late times (Itoh et al. 1993), is consistent with the model developed in Section 4.5. For this reason, Section 5.3 concluded that the multimass simulations are in strong support of the validity of the prescription for constructing merger histories described in Section 4.3, and of the accuracy of equation (52).

The distribution of the number of progenitors for a given clump size as a function of time (equation 52) provides valuable insight into the process by which hierarchical clustering develops. Fig. 8 shows this distribution for two choices of the final clump size k. The smaller value ($k = 10$) is chosen to represent those clumps that are of the same order of magnitude as the mean clump size, at the epoch corresponding to Δ_2. The larger value ($k = 10^4$) represents clumps that are much more massive than the characteristic (mean) mass – they are on the very high-mass tail of the Press–Schechter distribution. The figure shows the distribution of the number of progenitors, m, for these two, very different, clump sizes. For both values of k it shows the $n(m|k)$ distribution for four different choices of Δ_1 and Δ_2.

These epochs are chosen so that the difference in time between Δ_1 and Δ_2 is the same. That is, the curves represent choices of initial and final epochs that have the same 'look-back' time (see, e.g., Kauffmann 1995). For simplicity, the figure is constructed for an $\Omega = 1$ cosmology. As Section 2.3 shows, at late times (so that the second term in equation 25 can be neglected), $\Delta \approx (5a_i/3a) = (5/3)(t_i/t)^{2/3}$. Let dt denote the constant look-back time. Then, for sufficiently small values of $\Delta_1 = (5/3)(t_i/t_1)^{2/3}$, the later epoch in the figure is $\Delta_2 = (5/3)(t_i/[t_1 + dt])^{2/3}$. The figure was constructed with $t_i = 1$ and $dt = 50$. The solid curves show equation (52) for $\Delta_1 = 0.1$. The dashed curve shows the result when Δ_1 is the same as Δ_2 for the solid curve (the look-back time is still $dt = 50$). Similarly the dot-dashed and the dotted curves were constructed using the dashed and the dot-dashed values of Δ_2 as their values of Δ_1. Thus, in the figure, as Δ_1 and Δ_2 decrease, the curves shift towards the left. The open circle at the peak of each curve shows $n(m|k)$ at the mean value of m (as given by equation 53). The figure shows that this mean value is also the most probable.

For each curve, the mean clump size is $1 + (1/\Delta_2) \equiv 1/(1 - b_2)$. Fig. 8 shows that the curves that describe clumps that are slightly smaller than the mean clump size ($k = 10$) differ markedly from those that describe the extremely massive clumps ($k = 10^4$). Most of the smaller clumps have only one or two progenitors, and $n(m|k)$ does not depend strongly on the value of Δ_2. On the other hand, the distribution of the number of progenitors of the extremely massive clumps depends quite strongly on epoch. A massive clump at early times has, on average, many more progenitor clumps than at later epochs; the solid curve peaks at larger m than the dotted curve. This simply reflects the fact that, at earlier epochs, a massive clump must form from smaller objects, since the characteristic mass is smaller at that epoch. Fig. 8 also shows that the curves become broader at later epochs. This, too, is reasonable since, at later times (i.e., smaller Δ_2) and for a fixed look-back time, there is a greater dispersion around the mean progenitor size. Thus, Fig. 8 shows how the merger probabilities of Section 4.3 can quantify differences in the evolution of smaller clumps compared with very massive clumps.

The results of Sections 4.3 and 4.4 have another interesting application. Equation (52) gives the probability that a clump of

© Royal Astronomical Society • Provided by the NASA Astrophysics Data System

Downloaded from https://academic.oup.com/mnras/article/276/3/796/1034602 by U.S. Department of Justice user on 17 August 2022

1995MNRAS.276..796S

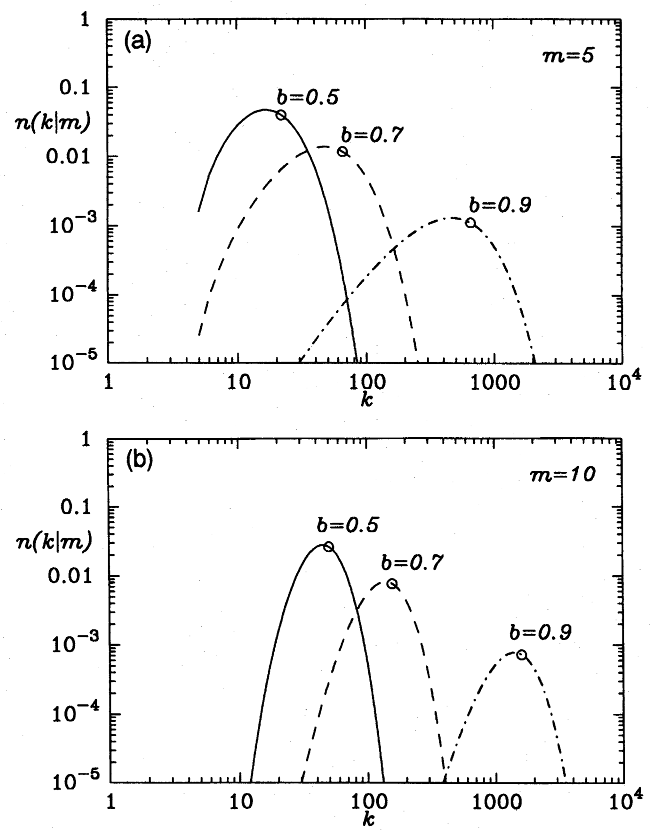

Figure 9. Estimate of the mass, k, for two values of the number of subclumps, m. The top panel shows $n(k|m)$ when $m=5$, and the lower panel shows these estimates when $m=10$. For both the plots, solid, dashed, and dash-dotted curves correspond to $b=0.5, 0.7$, and 0.9, respectively. The open circles near the peak of each curve show the mean value of the estimated mass (equation 64).

size k at the epoch Δ_2 had m progenitors at the epoch Δ_1. Therefore, the probability that a clump is of size k at the epoch Δ_2, given that it had m progenitors at the epoch Δ_1, is

$$n(k,\Delta_2|m,\Delta_1)=\frac{n(m,\Delta_1|k,\Delta_2)\eta(k,b_2)}{h(m;b_1,b_2)},\qquad \text{provided}\qquad k\geqslant m, \tag{62}$$

and is zero otherwise. This relation follows from Bayes' theorem, provided $h(m;b_1,b_2)$ is given by equation (57), and $\eta(N,b)$ is given by equation (2), with the usual relation (equation 19) between b and Δ. Note that as $\Delta_1\to\infty$, or as $b_1\to 0$, then $n(k,\Delta_2|m,\Delta_1)\to 1$ when $k=m$, and it tends to zero otherwise. This is the correct result because, when $b_1=0$, the distribution is Poisson; in this limit all progenitor clumps have one and only one particle.

The limit as $\Delta_1\to\Delta_2$ is also interesting because it can be interpreted analogously to the merger rate (equation 44) calculation derived in Section 4.1. Thus,

$$\lim_{\Delta_1\to\Delta_2} n(k,\Delta_2|m,\Delta_1)=\left(\frac{k^{k-1}b^{k-1}\mathrm{e}^{-kb}}{k(k-m)!}\right)\bigg/\left\langle\frac{(k-1)!}{(k-m)!}\right\rangle, \tag{63}$$

where $\Delta_1\to\Delta_2=\Delta$ so that $b_1\to b_2=b$, and where the denominator is the expectation value of the quantity in the angled brackets when it is averaged over the Borel distribution $\eta(N,b)$. Equation (63) denotes the probability that a clump with m progenitor subclumps is of size k, at the epoch Δ. Thus, equation (63) provides a way to estimate the size, k, of a clump when the number of subclumps is known, but the mass of each subclump is not. When $m=1$, then equation (63) reduces to $\eta(k,b)$, as it should. As m increases, the mean of this estimated mass is

$$\big\langle (k-1)(k-2)\dots(k-m+1)\big\rangle^{-1}\left(\sum_{k\geqslant m}^{\infty}k\,\frac{(k-1)!}{(k-m)!}\,\eta(k,b)\right)=\frac{\big\langle k(k-1)(k-2)\dots(k-m+1)\big\rangle}{\big\langle (k-1)(k-2)\dots(k-m+1)\big\rangle}. \tag{64}$$

The numerator in this expression is the mth factorial moment of the Borel distribution. The denominator can also be expressed in terms of factorial moments of the Borel distribution, so that, in principle, this mean estimated mass, given the number of subclumps, can be determined analytically.

Fig. 9 shows examples of these estimates for two values of the number, m, of subclumps. The top panel shows $n(k|m)$ when

© Royal Astronomical Society • Provided by the NASA Astrophysics Data System

Downloaded from https://academic.oup.com/mnras/article/276/3/796/1034602 by U.S. Department of Justice user on 17 August 2022

1995MNRAS.276..796S

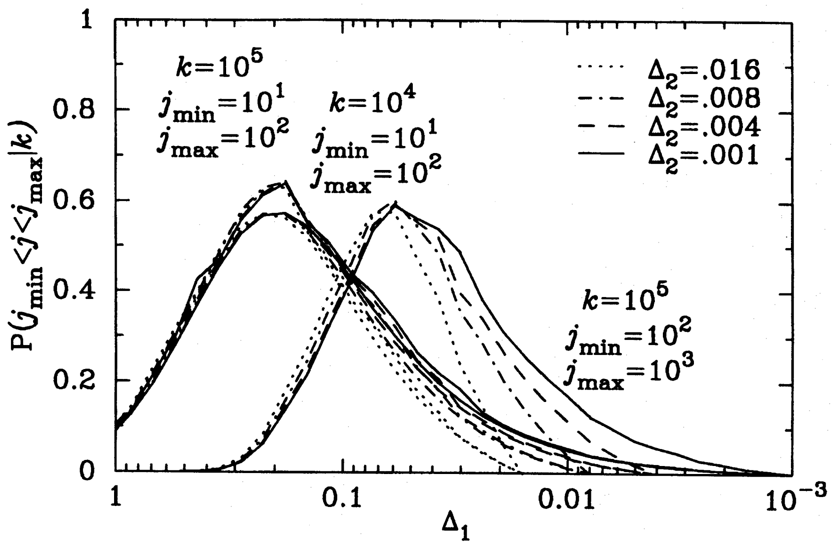

Figure 10. Mass fraction of k-clumps identified at Δ_2 that is in j-clumps at Δ_1, as a function of Δ_1, for a few representative values of k, Δ_2, $j_{\rm min}$, and $j_{\rm max}$.

$m = 5$, and the lower panel shows these estimates when $m = 10$. For both plots, solid, dashed, and dotted curves correspond to $b = 0.5, 0.7$, and 0.9, respectively. The open circles near the peak of each curve show the mean value of the estimated mass (equation 64). A number of features in these mass estimates are obvious. As m increases, the curves shift towards the right – the estimated mass increases as m increases. All curves are more strongly peaked at earlier epochs (smaller values of b). This is because the distribution around the mean mass is smaller at earlier epochs. At later epochs the curves become broader. Thus, at later epochs, the number of subclumps is not a very good indicator of the total mass.

Fig. 9 suggests that, at earlier epochs corresponding to higher redshifts, these estimates of the total mass may be compared with, for example, X-ray observations of substructure in clusters. Of course, observations are only likely to see subclumps that are greater than some minimum mass. Therefore, the estimates provided by equation (63) should be treated as lower bounds on the value of the total mass.

The Press–Schechter type model for the growth of hierarchical clustering considered in Sections 4.1 and 4.2 has an interesting implication for models of galaxy formation. Consider a model of structure formation in which stars burn only in objects of some small mass range, provided that those objects are themselves within larger clumps (e.g. Bower et al. 1993). Then, if star formation occurs only in clumps of size j, with $j_{\rm min} < j < j_{\rm max}$, provided that the j-clumps are within a larger clump of size k, then the mass fraction of the k-clump (identified at Δ_2) that is able to form stars at the earlier epoch Δ_1 is calculated as described at the end of Section 4.1.

Fig. 10 shows the mass fraction, $P(j_{\rm min} < j < j_{\rm max}|k)$, for a few representative choices of k, Δ_2, $j_{\rm min}$, and $j_{\rm max}$, as a function of Δ_1. Since the threshold Δ is related to the expansion factor, Fig. 10 is a scaled version of a plot of star formation versus time. Notice that, in this model, star formation peaks at a specific epoch in the history of the universe. The parameters in the figure are chosen to show that this epoch depends on $j_{\rm min}$ and $j_{\rm max}$, but is not so sensitive to the choice of k. Since star formation may release large quantities of heat, this result suggests that, if this model for structure formation is correct, then the thermal history of the universe may be strongly affected by hierarchical clustering. This result compliments and extends the analysis of the Butcher-Oemler effect studied by Bower (1991) and by Kauffmann (1995).

As mentioned in Section 4.3, each expression $p(l_1, \ldots, l_m|k)$ is a term in the partition function that describes all possible merger history trees. Although knowledge of the entire partition function is useful, it is usually the case that certain sums over the partition function are more useful than knowledge of the detailed structure of the partition function itself. For example, the Press–Schechter statements, $f(j|k)$, that describe the merging of trajectories are useful statements that correspond to particular sums over the partition function (cf. Section 4.3). Similarly, the statements $n(m|k)$ also provide coarse-grained information about the structure of the partition function. Other information that may be obtained by coarse-graining the partition function includes, for example, statements about the mean progenitor clump size, and the dispersion about that mean size, for a given final clump size. Such statements provide information about the relative likelihood that a given clump formed primarily by mergers of equal-sized objects, or by the accretion of smaller objects by a massive one. The evaluation of statements such as these will be reserved for a future publication.

To derive a counts-in-cells distribution function from the Press–Schechter multiplicity function requires knowledge of the spatial distribution and the internal substructure of the Press–Schechter clumps. In the present work, which treated the case of an initially Poisson distribution, the Press–Schechter (Borel) clumps were assumed to be point-sized and to have a Poisson spatial

Downloaded from https://academic.oup.com/mnras/article/276/3/796/1034602 by U.S. Department of Justice user on 17 August 2022

© Royal Astronomical Society • Provided by the NASA Astrophysics Data System

1995MNRAS.276..796S

distribution. The extension to clumps that have non-trivial shapes is straightforward (Sheth & Saslaw 1994). The other assumption, that the Press–Schechter clumps initially have a Poisson spatial distribution, finds very strong support from the scaling solution derived in Section 3.2. Furthermore, a linear theory analysis of clustering from an initially Poisson distribution (Section 2.3; Peebles 1980, section 70) also implies this same result. In any case, the PPSD counts-in-cells distribution function that results from this assumption about the spatial distribution of the Press–Schechter clumps provides an excellent description of the $f(N)$ distribution measured in N-body simulations of gravitational clustering. Given the good agreement of the Borel multiplicity function with the cluster multiplicity function measured in the simulations (Fig. 6), the good agreement of the PPSD with the counts-in-cells distribution functions measured in the simulations justifies the assumption that the Press–Schechter Borel clumps have a Poisson spatial distribution.

Moreover, for this special case of clustering from an initially Poisson distribution, many details of the structure of the partition function of the merger history tree can also be obtained (Section 4.3). This partition function, when combined with the assumption that the Press–Schechter Borel clumps identified at a given epoch initially have a Poisson spatial distribution at that epoch, provides a detailed description of the growth of hierarchical clustering on all levels of the hierarchy (Section 4.5). In this sense, the Press–Schechter description of the growth of hierarchical clustering from an initially Poisson distribution is, essentially, complete. Although many of the details of the growth of clustering from an initially Poisson distribution are now known, it is unlikely that a Poisson distribution is an accurate model of the initial conditions for gravitational clustering in our universe. At present, however, analytic understanding of the growth of clustering from more general Gaussian initial conditions is not as detailed as for the Poisson case studied here. Nevertheless, the close relation of the Poisson distribution to a white noise Gaussian suggests that many of the results obtained in this paper should provide at least qualitative insight into the evolution of clustering from more general initial conditions.

To extend these results (for the clustering of the initial particles, and also for the clustering of Press–Schechter clumps) to the case of an initially Gaussian distribution requires knowledge of the Press–Schechter multiplicity function for the Gaussian distribution (which is known), and also knowledge of how those clumps are distributed (which is not). There are two main reasons why the Press–Schechter description of an initially Poisson distribution is more tractable than it is for the more general initially Gaussian random density field. The first is technical: whereas the multiplicity function for an initially Gaussian random field has been calculated, the low-mass tail diverges (e.g. Press & Schechter 1974; Bond et al. 1991). For a discrete Poisson distribution, on the other hand, there is a lowest mass clump – a single particle. This means that statements such as 'the number of progenitor clumps for a given clump size' that are useful and meaningful for an initially Poisson distribution must be replaced by statements like 'the number of progenitor clumps that are larger than some given mass, for a given clump size'. These statements are more difficult to formulate. However, in practice, most Press–Schechter statements are tested using N-body simulations, and, at present, such simulations have a lower limit to the mass resolution they can probe. If this lowest mass scale is treated as the 'mass of a single particle', then it may be that the techniques used here, which depend essentially on the combinatorics of integers, will be useful for the Gaussian case also.

The second reason why the Poisson case is easier to solve involves the spatial distribution of the Press–Schechter clumps. Whereas the scaling solution of Section 3.2 strongly suggests that the Poisson Press–Schechter clumps identified at a given epoch initially have a Poisson spatial distribution at that epoch, there is, at present, no way to describe the spatial distribution of the Press–Schechter clumps for an initially Gaussian random field. One possible solution to this problem is to make an assumption about the spatial distribution of the Press–Schechter clumps by drawing an analogy to the analytic result for the Poisson case: namely, assume that the Press–Schechter clumps themselves have a Gaussian distribution with a power spectrum that is consistent with that required by linear theory. This approach is presently under investigation. However, studies of the peaks of Gaussian random fields (e.g. Rice 1944, 1945; Kaiser 1984; Bardeen et al. 1986; Jensen & Szalay 1986) strongly suggest that, although Press–Schechter clumps are not so trivially related to these peaks, the spatial distribution of the clumps is not easily related to the linearly evolved power spectrum. Furthermore, if the initial density distribution is Gaussian, then, in contrast to the case of an initially Poisson distribution, it is likely that the positions of minima in the initial potential (when smoothed on very large scales) will not be good tracers of the (smoothed, large-scale) potential minima at late times. If this last effect is termed dynamical clustering, then the Press–Schechter description can be thought of as describing only that part of the clustering that is due entirely to the statistics of the initial density field. For this reason, Bond & Myers (1993) use a combination of the Press–Schechter approach and the peaks formalism to describe statistical clustering, and then use the Zel'dovich approximation to describe the dynamical clustering of the peaks, to tackle this difficult problem of describing, more exactly, the evolution of the spatial distribution of the Press–Schechter clumps. Although the Bond & Myers approach is a valuable first step, extending the results obtained in this paper to general Gaussian random fields remains an unsolved problem.

Given these difficulties in converting Press–Schechter multiplicity functions for more general (non-Poisson) initial conditions into counts-in-cells distribution functions, it is very interesting that the PPSD (equation 1) derived in this paper provides a very good fit to the distribution function of galaxy counts in randomly placed cells measured in a number of optical and infrared catalogues (Sheth et al. 1994, and references therein). Since the Press–Schechter mass functions for arbitrary initial Gaussian density distributions (e.g. Gaussian distributions with the standard cold dark matter initial spectrum) are closely related to the Borel multiplicity function for the Poisson distribution considered here, and from which the PPSD is derived, and since the galaxy

Downloaded from https://academic.oup.com/mnras/article/276/3/796/1034602 by U.S. Department of Justice user on 17 August 2022

© Royal Astronomical Society • Provided by the NASA Astrophysics Data System

1995MNRAS.276..796S

catalogues presently available only sparsely sample the underlying density field, it is incorrect to assume that the agreement of the PPSD with observations supports the case for Poisson initial conditions. The sparseness of the sampling precludes a definitive statement in this regard. On the other hand, the measured agreement of the PPSD and the observations does suggest that the Press–Schechter type description of non-linear clustering, which appears to provide a good description of gravitational clustering in relevant N-body simulations, is in general agreement with observations. Therefore, we conclude by noting that the measured good agreement between equation (1) and observations of optical and infrared galaxies, and the relation, derived in this paper, between this counts-in-cells distribution and the non-linear clustering model of Press & Schechter, provides strong observational evidence for the validity of the Press–Schechter approach.

ACKNOWLEDGMENTS

I thank the Marshall Aid Commemoration Commission for a Marshall Scholarship, the Institute of Astronomy and Jesus College, Cambridge, for financial support, Marc Davis and the Berkeley Astronomy Department for their hospitality, and Gerard Lemson, Xiaochun Luo, Guinevere Kauffmann, and Simon White for interesting and encouraging discussions.

REFERENCES

Abel N. H., 1826, Crelle, 1, 159
Abramowitz M., Stegun I. A., 1964, Handbook of Mathematical Functions. National Bureau of Standards, Applied Mathematics Series, 55
Adler R. J., 1981, The Geometry of Random Fields. Wiley, New York
Bardeen J. M., Bond J. R., Kaiser N., Szalay A. S., 1986, ApJ, 304, 15
Bernardeau F., 1994, ApJ, 427, 51
Bond J. R., Cole S., Efstathiou G., Kaiser N., 1991, ApJ, 379, 440
Bond J. R., Myers S., 1993, preprint, CITA
Bower R., 1991, MNRAS, 248, 332
Bower R., Coles P., Frenk C., White S. D. M., 1993, ApJ, 405, 403
Consul P. C., 1989, Generalized Poisson Distributions: Properties and Applications. M. Dekker, New York
Davis M., Peebles P. J. E., 1977, ApJS, 34, 425
Epstein R. I., 1983, MNRAS, 205, 207
Hamilton A. J. S., 1988, ApJ, 332, 67
Hamilton A. J. S., Saslaw W. C., Thuan T. X., 1985, ApJ, 297, 37
Itoh M., Inagaki S., Saslaw W. C., 1988, ApJ, 331, 45
Itoh M., Inagaki S., Saslaw W. C., 1993, ApJ, 403, 459
Jensen L. G., Szalay A. S., 1986, ApJ, 305, L5
Kaiser N., 1984, ApJ, 284, L9
Kauffmann G., 1995, MNRAS, 274, 153
Kauffmann G., White S. D. M., 1993, MNRAS, 261, 921
Lacey C., Cole S., 1993, MNRAS, 262, 627
Lacey C., Cole S., 1994, MNRAS, 271, 676
Lahav O., Saslaw W. C., 1992, ApJ, 396, 430
Lucchin F., Matarrese S., 1988, ApJ, 330, 535
Moran P. A. P., 1984, An Introduction to Probability Theory. Oxford Univ. Press, Oxford
Peebles P. J. E., 1980, The Large Scale Structure of the Universe. Princeton Univ. Press, Princeton
Press W. H., Schechter P., 1974, ApJ, 187, 425
Rephaeli Y., Saslaw W. C., 1986, ApJ, 309, 13
Rice S. O., 1944, Bell Sys. Tech. J., 23, 282
Rice S. O., 1945, Bell Sys. Tech. J., 24, 41
Riordan J., 1979, Combinatorial Identities. Robert E. Krieger Publ. Co., New York
Saslaw W. C., 1985, ApJ, 297, 49
Saslaw W. C., 1989, ApJ, 341, 588
Saslaw W. C., Crane P., 1991, ApJ, 380, 315
Saslaw W. C., Hamilton A. J. S., 1984, ApJ, 276, 13
Schechter P., 1976, ApJ, 203, 297
Sheth R. K., 1994, PhD thesis, Cambridge University
Sheth R. K., Saslaw W. C., 1994, ApJ, 437, 35
Sheth R. K., Mo H. J., Saslaw W. C., 1994, ApJ, 427, 562
Suto Y., Itoh M., Inagaki S., 1990, ApJ, 350, 492
Szapudi I., Szalay A., 1993, ApJ, 408, 43
White S. D. M., Frenk C., 1991, ApJ, 379, 52
Zhan Y., 1989, ApJ, 340, 23

This paper has been produced using the Royal Astronomical Society/Blackwell Science LaTeX style file.

Downloaded from https://academic.oup.com/mnras/article/276/3/796/1034602 by U.S. Department of Justice user on 17 August 2022

© Royal Astronomical Society • Provided by the NASA Astrophysics Data System